Paleocene to Miocene southern Tethyan carbonate factories of the Southwestern and Western Central Asia

Coletti Giovanni[1,*]; giovanni.coletti@unimib.it

Commissario Lucrezi[1]; l.commissario@campus.unimib.it

Mariani Luca[1,2]; l.mariani35@campus.unimib.it

Bosio Giulia[1]; giulia.bosio@unimib.it

Soldi Mara[3]; mara.soldi@ecopetrolsrl.it

Bialik M. Or[4]; OBialik@gmail.com

1: Department of Earth and Environmental Sciences, University of Milano-Bicocca, Piazza della Scienza 4, 20126 Milano, Italy.

2: Departamento de Biologia, Universitat de les Illes Balears, Cra de Valldemossa, Km 7.5, 9, 07122 Palma de Mallorca, Spain.

3: Ecopetrol srl., Via Venanzio Buzzi 4, 20017 Rho, Italy.

4: Marine Geology & Seafloor Surveying, Department of Geosciences, University of Malta, Msida, MSD 2080, Malta

This is a non-peer reviewed preprint submitted to EarthArXiv, the manuscript has been submitted to The Depositional Record on the 11/03/2022.

Paleocene to Miocene southern Tethyan carbonate factories of the Southwestern and Western Central Asia

Coletti Giovanni[1,*]

Commissario Lucrezi[1]

Mariani Luca[1,2]

Bosio Giulia[1]

Soldi Mara[3]

Bialik M. Or[4]

1: Department of Earth and Environmental Sciences, University of Milano-Bicocca, Piazza della Scienza 4, 20126 Milano, Italy.

2: Departamento de Biologia, Universitat de les Illes Balears, Cra de Valldemossa, Km 7.5, 9, 07122 Palma de Mallorca, Spain.

3: Ecopetrol srl., Via Venanzio Buzzi 4, 20017 Rho, Italy.

4: Marine Geology & Seafloor Surveying, Department of Geosciences, University of Malta, Msida, MSD 2080, Malta.

*: corresponding author, giovanni.coletti@unimib.it

Abstract

One hundred and forty-four sections of shallow-water carbonates, deposited between the Paleocene and the Miocene, from the Levant to the Himalaya, have been investigated to analyze the distribution of carbonate facies and carbonate producing organisms. Large benthic foraminifera resulted the volumetrically most important group of carbonate producers during the whole period, with a peak in abundance during the Eocene. Colonial corals are relatively abundant during the Paleocene and in the Miocene, their abundance peak during the Oligocene and has a minimum during the Eocene. Red calcareous algae have a similar pattern although their peak in abundance covers both the Oligocene and the Miocene. Green calcareous algae decrease from the Paleocene onward. Facies related to very shallow and/or restricted marine conditions peak during the Miocene and in particular during the Aquitanian. Both the pattern of large benthic foraminifera and of colonial corals seems to be related to temperatures, with warm periods favoring the former and cool periods the latter. Red calcareous algae display a pattern similar to that of colonial corals suggesting that the periods favorable for one group, on the large scale, are also favorable for the other. The progressive decrease of green calcareous algae could be tentatively related to a preservation bias connected to the transition from Paleogene assemblages that included presumably calcitic taxa of green algae and Neogene assemblages entirely constituted by aragonitic taxa with limited preservation potential. The Aquitanian peak in facies related to very shallow and/or restricted marine conditions is most likely connected to the progressive narrowing of the Tethys related to the collision between Arabia and Eurasia. These results denote an overall agreement between the abundance of the various types of shallow-water carbonate facies and large-scale environmental and geological processes, highlighting the potential for paleoenvironmental reconstruction locked in the shallow-water record.

Keywords: Reefs, corals, calcareous algae, large benthic foraminifera, Asmari Formation, Qom Formation.

1. Introduction

Earth's biosphere is the result of a complex and ever-changing balance. Biomes can migrate geographically, expand, recede or disappear entirely with new ones arising to take their place. These shifts in environments and their inhabitants have been recorded in the fossil record. However, while many biomes leave limited trace of their existence, others, like tropical carbonate factories, produce massive sedimentary successions that testify on their evolution trough time. Carbonate factories represent both the space where biological carbonate sediments are produced and the associations of carbonate producing organisms (Tucker and Wright, 1990; Wright and Burchette, 1996; Schlager, 2003). Since a sizable share of benthic organisms inhabiting the biomes of the carbonate factories (e.g., corals, mollusks, calcareous algae, foraminifera) possess a mineralized skeleton, generally either calcite, aragonite or a combination of both, their remains have an high preservation potential and can accumulate in rock-forming quantities. Thanks to this massive and widespread fossil record it is possible to use carbonate factories as a proxy for studying the changes in the climate of the planet through time (e.g., Halfar and Mutti, 2005; Bosellini and Perrin, 2008; Wilson, 2008; Perrin and Bosellini, 2012; Perrin and Kiessling, 2012; Pomar et al., 2017). Carbonate factories distribution and their paleoenvironmental implications have been extensively reviewed at both regional and global scale (e.g. Kiessling et al., 1999; Kiessling et al., 2002; Halfar and Mutti, 2005; Nebelsick et al., 2005; Johnson et al., 2008; Pomar et al. 2017). However, these studies often encounter two main limitations. The first is the lack of quantitative data, which significantly hinders any large-scale analysis and accurate comparison of sedimentary successions. The second limitation relates to the geographic distribution of case studies, with the overwhelmingly majority of well-studied carbonate successions being located in the European area for historical reasons.

Here we strive to try to overcome both of these limitations by compiling a database that summarizes the distribution of Cenozoic carbonate facies of the Southwestern and Western Central

Asia. With this database, we aim to reconstruct the large-scale patterns and discuss their paleoenvironmental implications. This vast region of the world is characterized by extensive carbonate successions deposited during the Cenozoic in the shallow water of the Tethys. The presence of large hydrocarbon reservoirs in these successions (especially in Iran; Perry and Choquette, 1985; Amirshankarami et al., 2007; Coletti et al., 2017) provides us with a trove of information scattered in individual publications which have not been considered in a larger framework. These papers provide a sizable and invaluable dataset for the investigation of the distribution of carbonate factories and carbonate producers, and to better grasp the global evolution of shelfal biomes during the Cenozoic.

2. Geological context

The region referred to here as the Southwestern and Western Central Asia consists of landmasses mostly located south of the suture line between the African-Arabian and Indian plates and the Eurasian plate (Fig. 1). During the Paleocene to early Miocene, this area was occupied by part of the Tethys, the ocean that separated the African, Arabian and Indian landmasses (Gondwanian derived fragments) in the South from the Eurasia in the North (Fig. 1). During the entirety of the investigated period (Paleocene – Miocene) the Tethys was mainly located at tropical latitudes (Rögl, 1999; Dercourt et a., 2000; Scotese, 2014a, b). This, combined with an overall warm climate punctuated by extremely warm spikes during the early Paleogene (Zachos et al., 2001; Barnet et al., 2019; Miller et al., 2020), favored the deposition along Tethys' shelves of shallow-water carbonates (and, at times, evaporites) through most of the investigated time-interval. These carbonates formed in a wide variety of environments, ranging from open shelves to restricted embayments and from nutrient-rich to oligotrophic settings, providing a comprehensive overview of the various types of carbonate factories of the Cenozoic.

The northward movement of the African, Arabian and Indian landmasses caused the progressive closure of the Tethys (Robertson et al., 2012; Garzanti et al., 2016; Hu et al., 2016). The initial collision

between the Indian and Eurasian plate took place around 60-61 Ma (Hu et al., 2016; An et al., 2021), leading to the end of marine sedimentation in Tibet and in the Indus Basin (i.e. the western part of the study area) during the Eocene (Blondeau et al., 1986; Afzal et al., 2009, 2010; Ahmad et al. 2016) (Fig. 1). The collision between the Arabian and Eurasian plates probability initiated during the latest Eocene – early Oligocene and was entirely completed before ca. 14 Ma (middle Miocene) (Ballato et al., 2010; Agard et al., 2011; Cornacchia et al., 2018; Bialik et al., 2019; GholamiZadeh et al., 2021), leading to the end of marine sedimentation in most of the Mesopotamian and Iranian regions (i.e., the central part of the study area) during the Miocene (Ziegler, 2001; Al-Juboury and McCann, 2008; Mossadegh et al., 2009; Reuter et al., 2009; Mohammadi et al., 2013; Sissakian, 2013; Ameen-Lawa and Ghafur, 2015; Sadooni and Alsharhan, 2019) (Fig. 1). The Arabian and Levant regions (i.e., the eastern and central part of the study area), during the late Eocene - Oligocene, were also affected by a regional uplift testified by large hiatuses (Alsharhan and Nairn, 1995; Whittle et a., 1995; Buchbinder et al., 2005; Al-Juboury and McCann, 2008; Agard et al., 2011; Avni et al., 2012; Farouk et al., 2013; Bernecker, 2014; Coletti et al., 2019; Sadooni and Alsharhan, 2019). This event has been related to the development of the Afar Dome and the opening of the Red Sea (Ziegler, 2001; Avni et al., 2012; Bernecker, 2014). Both geodynamic processes progressively effected the marine environments of the Tethys that are now exposed as outcrops in this vast area running from western Tibet to the southeastern Mediterranean.

3. Material and methods

In order to prepare the database, the main online repositories (Google Scholar; Scopus) were searched for papers dealing with the Cenozoic carbonate successions of Egypt, Cyprus, Israel, Jordan, Saudi Arabia, United Arab Emirates (UAE), Yemen, Oman, Iraq, Iran, Pakistan, India, Nepal and China (Tibet). To be included into the database a paper needed to fulfill the following requirements: 1) a lithostratigraphic description of a section completed with a lithostratigraphic column; 2) facies descriptions, including a qualitative or quantitative assessment of the main carbonate producers; 3)

information on facies distribution within the investigated section; 4) microphotographs of the recognized facies suitable for double checking facies descriptions; 5) a biostratigraphic or chronostratigraphic framework; 6) a reasonably accurate location of the investigated section.

The facies described in the selected papers were analyzed based on the abundance of the following categories of carbonate grains: free-living larger benthic foraminifera (LBF), encrusting benthic foraminifera (EBF), smaller benthic foraminifera (SBF), red calcareous algae (RCA), green calcareous algae (GCA), colonial corals (CC), mollusks, echinoderms, bryozoans, ostracods, microbial crusts, ooids, peloids and carbonate mud. Each facies was reclassified based on its dominant component (e.g. RCA dominated), or on its codominant components (e.g. RCA & LBF dominated). Facies dominated by terrigenous grains, pelagic material or evaporites, where excluded from the analysis.

Each section included into the database was subdivided into fractions at epoch level (e.g. Eocene, Oligocene) and, wherever possible, at stage level (e.g., Ypresian, Lutetian). Within each fraction of a section the abundance of each recognized facies was calculated based on how many meters of the fraction are characterized by the facies (e.g., a 40 m fraction of section, deposited during the Ypresian, consists of 20 m of LBF dominated packstone and of 20 m of ooids dominated grainstone, thus the fraction consists of 50% of LBF dominated facies and 50% of ooids dominated facies). The raw data are available as supplementary material (Supplementary Table 1).

The data have been grouped based on two different approaches: section average and formation average. With the section average approach, the averages are calculated as the average of each fraction belonging to the same time slice (e.g., the average of all Miocene-aged fractions of sections; the average of all Burdigalian-aged fractions of sections). With the formation average approach, the averages of all the fractions of sections belonging to the same formation and the same time slice are calculated and then a general average is provided.

This analysis can be affected by two main biases, the first related to the reliability of the original information and the second related to the geographic distribution of the sections included into the database. The former bias has been partially countered by cross checking both facies descriptions and biostratigraphic information and focusing only on those elements of the facies that were 1) described as dominant and 2) appeared as dominant also in the microphotographs included in the source material. The geographic distribution of the sections is strongly related to the geological setting. While Paleocene and Eocene sections are more or less evenly distributed into the study area, Oligocene and Miocene sections mainly occur in the Iraq-Iran area (Fig. 1A). This is mainly related to the progressive closure of the Tethys due to the collision of the Indian and African-Arabian plates with Eurasia, which results in the lack of shallow-water carbonate successions in several regions during the Oligocene-Miocene (e.g., Tibet). This geographical bias has been partially countered by proposing both a section-average and a formation-average for each time interval. The section-average approach clearly indicates the average volume of a certain facies among the investigated carbonate successions. This approach provides quantitative data but can over-represents certain areas where there are more investigated outcrops per square kilometer (e.g., the Asmari and Qom formations of Iran during the Oligo-Miocene interval). The formation average approach partially solves this problem by averaging the data from each formation, thus reducing the overrepresentation of certain areas. Neither the geographic nor the reliability bias can be entirely solved and must be taken into account when approaching a paleoenvironmental interpretation of the results.

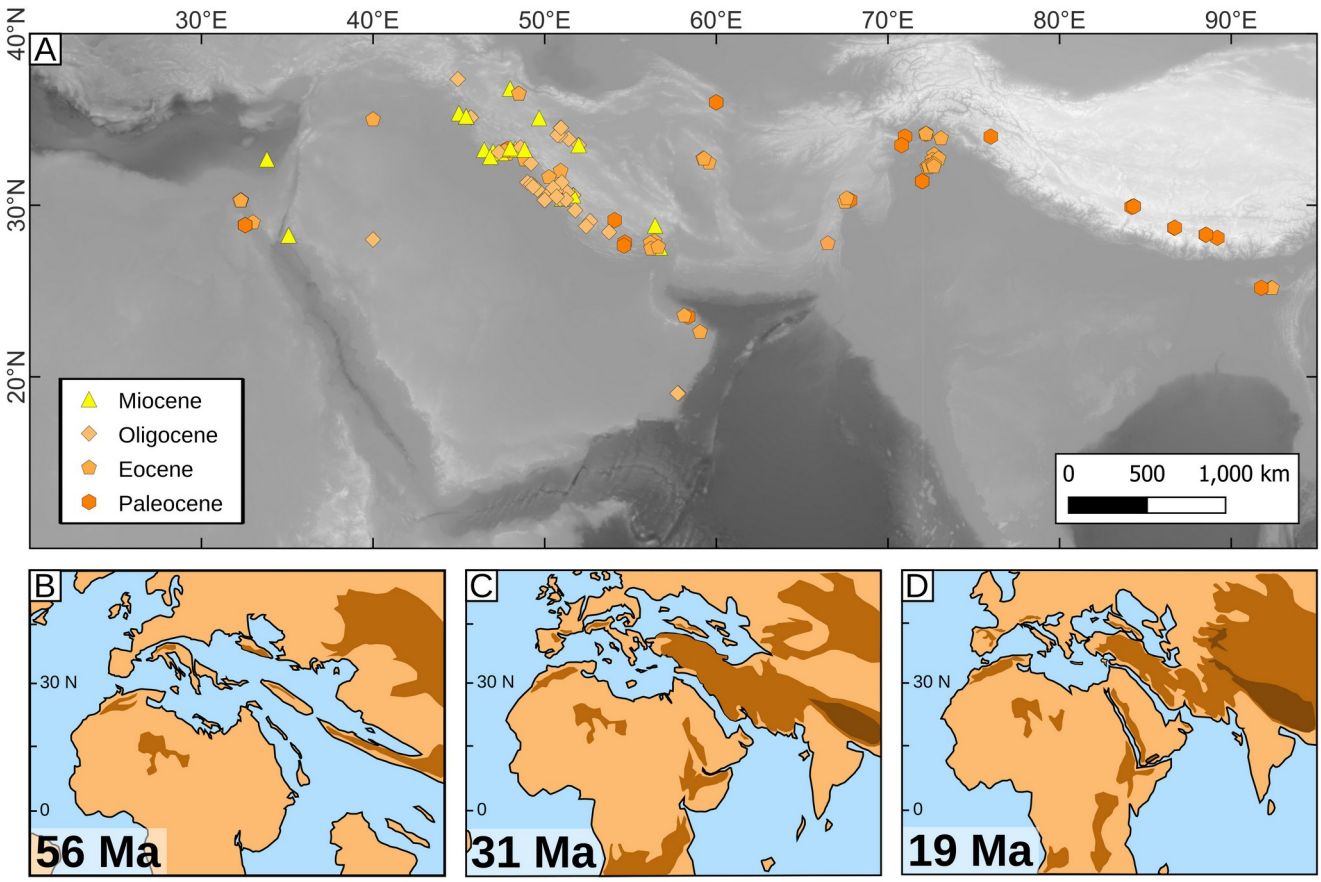

Figure 1. Geographic locations of the studied facies and paleogeographic reconstructions. A. Geographic location of the fossil Neogene facies investigated in this study. Note the different symbols and colors for different epochs. All the references are reported in Supplementary Table 1. B. Paleogeographic reconstruction of the Southwestern and Western Central Asia about 56 Ma (Paleocene-Eocene), after Scotese (2014a, b). C. Paleogeographic reconstruction of the Southwestern and Western Central Asia about 31 Ma (early Oligocene), after Scotese (2014a, b). D. Paleogeographic reconstruction of the Southwestern and Western Central Asia about 19 Ma (early Miocene), after Scotese (2014a, b).

#	Reference	Country	Formation	Stratigraphic range	N. of sections
1	Rahmani et al., 2009	Iran	Asmari	Chattian - Burdigalian	1
2	Adabi et al., 2008	Iran	Taleh Zang	Lutetian - Bartonian	2
3	Roozpeykar & Moghaddam, 2016	Iran	Asmari	Rupelian - Burdigalian	1
4	Nafarieh et al., 2012	Iran	Jahrum	Selandian - Ypresian	2
5	Mahyad et al., 2019	Iran	Qom	Aquitanian - Burdigalian	2
6	Moghaddam et al., 2002	Iran	Jahrum & Pabdeh	Ypresian	1
7	Heidari et al., 2014	Iran	Mishan (Guri Member)	Aquitanian - Langhian	2
8	Shabafrooz et al., 2015	Iran	Asmari	Rupelian - Burdigalian	9
9	Vaziri-Moghaddam et al., 2006	Iran	Asmari	Chattian - Burdigalian	1
10	Zohdi et al., 2013	Iran	Jahrum	Ypresian - Bartonian	4
11	Daraei et al., 2015	Iran	Asmari	early Miocene	3
12	Roozpeykar et al., 2019	Iran	Asmari	Burdigalian	1
13	Avarjania et al., 2015	Iran	Asmari	Chattian - Burdigalian	4
14	Bagherpour & Vaziri, 2012	Iran	Taleh Zang	Thanetian - Ypresian	2
15	Amirshahkarami & Zebarjadi, 2018	Iran	Jahrum	Thanetian - Ypresian	1
16	Zoeram et al., 2015	Iran	Asmari	Rupelian - Burdigalian	1
17	Basso et al., 2019	Iran	Qom	Rupelian	1
18	Mohammadi et al., 2011	Iran	Qom	Chattian	1
19	Hadi et al., 2016	Iran	Ziarat	Ypresian - Bartonian	3
20	Sadeghi et al., 2011	Iran	Asmari	Rupelian - Chattian	3
21	Amirshahkarami, 2013	Iran	Asmari	Rupelian - Aquitanian	2
22	Vaziri-Moghaddam et al., 2010	Iran	Asmari	Chattian - Burdigalian	4
23	Amirshahkarami & Karavan, 2015	Iran	Qom	Rupelian - Burdigalian	1
24	Dill et al., 2018	Iran	Asmari	Rupelian - Burdigalian	5
25	Dill et al., 2012	Iran	Asmari	Chattian - Burdigalian	1
26	Noorian et al., 2021	Iran	Asmari	Rupelian - Burdigalian	3
27	Safari et al., 2020	Iran	Qom	Rupelian - Chattian	2
28	Amirshahkarami et al., 2007	Iran	Asmari	Rupelian - early Miocene	1
29	Babazadeh & Alavi, 2013	Iran	Lut platform	Ypresian	3
30	Taheri et al., 2008	Iran	Jahrum	Lutetian	1
31	Mossadegh et al., 2009	Iran	Asmari	Chattian - Burdigalian	2
32	Amirshahkarami et al., 2007	Iran	Asmari	Chattian - early Miocene	1
33	Adabi et al., 2016	Iran	Asmari	Rupelian - Burdigalian	1
34	Vaziri-Moghaddam et al., 2011	Iran	Asmari	Rupelian - Chattian	1
35	Mahboubi et al., 2001	Iran	Chehel- Kaman	Thanetian	2
36	Mohammadi, 2020	Iran	Qom	Rupelian - Burdigalian	2
37	Joudaki et al., 2020	Iran	Asmari	Rupelian - Burdigalian	2
38	Al-Qayim et al., 2016	Iraq	Bajwan, Anah, Euphrates, Jeribe	Rupelian - Burdigalian	1
39	Hussein et al., 2017	Iraq	Euphrates, Jeribe	Aquitanian - Burdigalian	5
40	Swati et al., 2013	Pakistan	Margalla Hill Limestone	Ypresian	1
41	Afzal et al., 2011	Pakistan	Lockhart, Patala, Dungan	Thanetian - Ypresian	5
42	Fahad et al., 2021	Pakistan	Chorgali	Ypresian	1
43	Ishaq et al., 2019	Pakistan	Sakesar Limestone	Ypresian	2
44	Ghazi et al., 2020	Pakistan	Nammal	Ypresian	6

45	Hanif et al., 2014	Pakistan	Lockhart	Thanetian	3
46	Ahmad et al., 2020	Pakistan	Dungan	Thanetian - Ypresian	1
47	Kamran et al., 2021	Pakistan	Patala	Thanetian - Ypresian	1
48	Kahsnitz, 2017	India	Spanboth, Zhepure Shan, Zongpu, Langzhu	Selandian - Ypresian	5
49	Sarkar, 2016	India	Umlatdoh (Umlatdoh Limestone)	Ypresian	1
50	Sarkar, 2017	India	Prang	Lutetian - Bartonian	1
51	Banerjee et al., 2018	India	Furla Limestone, Maniyara Fort	Lutetian - Bartonian, Chattian	2
52	Jahuri et al., 2006	India	Lakadong (Lakadong Limestone)	Thanetian	1
53	Jiang et al., 2021	China	Jialazi	Thanetian - Ypresian	2
54	Li et al., 2015	China	Zongpu	Danian - Ypresian	2
55	Li et al., 2020	China	Not reported (probably Zhepure Shan)	Thanetian - Ypresian	1
56	Willems et al., 1996	China	Zhepure Shan	Danian - Lutetian	1
57	Mattern & Bernecker, 2019	Oman	Jafnayn	Thanetian - Ypresian	1
58	Tomás et al., 2016	Oman	Jafnayn	Ypresian	1
59	Beavington-Penney et al., 2006	Oman	Seeb	Lutetian - Bartonian	1
60	Reuter et al., 2008	Oman	Shuwayr, Warak, Ghubbarrah	Rupelian - Aquitanian	2
61	Al-Kahtany, 2017	Saudi Arabia	Jabal Kibrit (Wadi Waqb Member)	middle Miocene	1
62	Corlett et al., 2018	Egypt	Hammam Faraun fault block	Ypresian - Lutetian	1
63	Sallam et al., 2015	Egypt	Minia, Sannor, Maadi	Ypresian, Bartonian - Priabonian	5
64	Scheibner et al., 2000	Egypt	Southern Galala	Thanetian	6
65	Scheibner et al., 2003	Egypt	Southern Galala	Thanetian	4
66	Coletti et al., 2019	Cyprus	-	early Miocene -late Miocene	1

Table 1: Summary list of the papers considered in this work, reporting references, countries, formations, stratigraphic ranges and the number of sections analyzed in the work. See Supplementary Table 1 for a complete dataset.

4. Results

Some 114 papers providing information on shallow water carbonate facies from the Paleocene to the Miocene were identified. Based on the aforementioned requirements, 66 papers and 144 sections, from Cyprus, Egypt, Saudi Arabia, Oman, Iraq, Iran, Pakistan, India and China were included into the database (Table 1; Supplementary Table 1; the database is also accessible online, https://doi.org/10.6084/m9.figshare.19323821.v1). The remaining papers, although providing qualitative data on the distribution of the main carbonate producers, lacked quantitative information on facies distribution throughout the described sections. The information from this latter group of papers was still included into the discussion.

The sections included into the database range in age from the Paleocene to the Miocene. The Paleocene is represented (in order of abundance) by the Thanetian, Danian and Selandian. As the database largely consists of shallow-water carbonates, the stratigraphic framework is strongly based on LBF biostratigraphy. Since LBF zonation is poorly constrained in the Danian-Selandian interval (e.g., Serra-Kiel et al., 1998), the pre-Thanetian stratigraphic framework is not well defined. The Eocene is largely represented by the Ypresian stage. Both stages of the Oligocene and both stages of the early Miocene are well represented within the database. On the other hand, the middle and late Miocene are poorly represented.

4.1 Epochs

Photozoan facies (sensu James, 1997), i.e. those dominated by CC, GCA, LBF, and RCA, dominate the carbonate successions of the study area, during the whole Paleocene-Miocene interval (Table 2; Fig. 2). Heterozoan facies (sensu James, 1997), i.e. those facies mainly dominated by heterotroph carbonate producers like mollusks, echinoderms, SBF, and bryozoans, are less common; their combined abundance peaks during the Miocene (Table 2; Fig. 2).

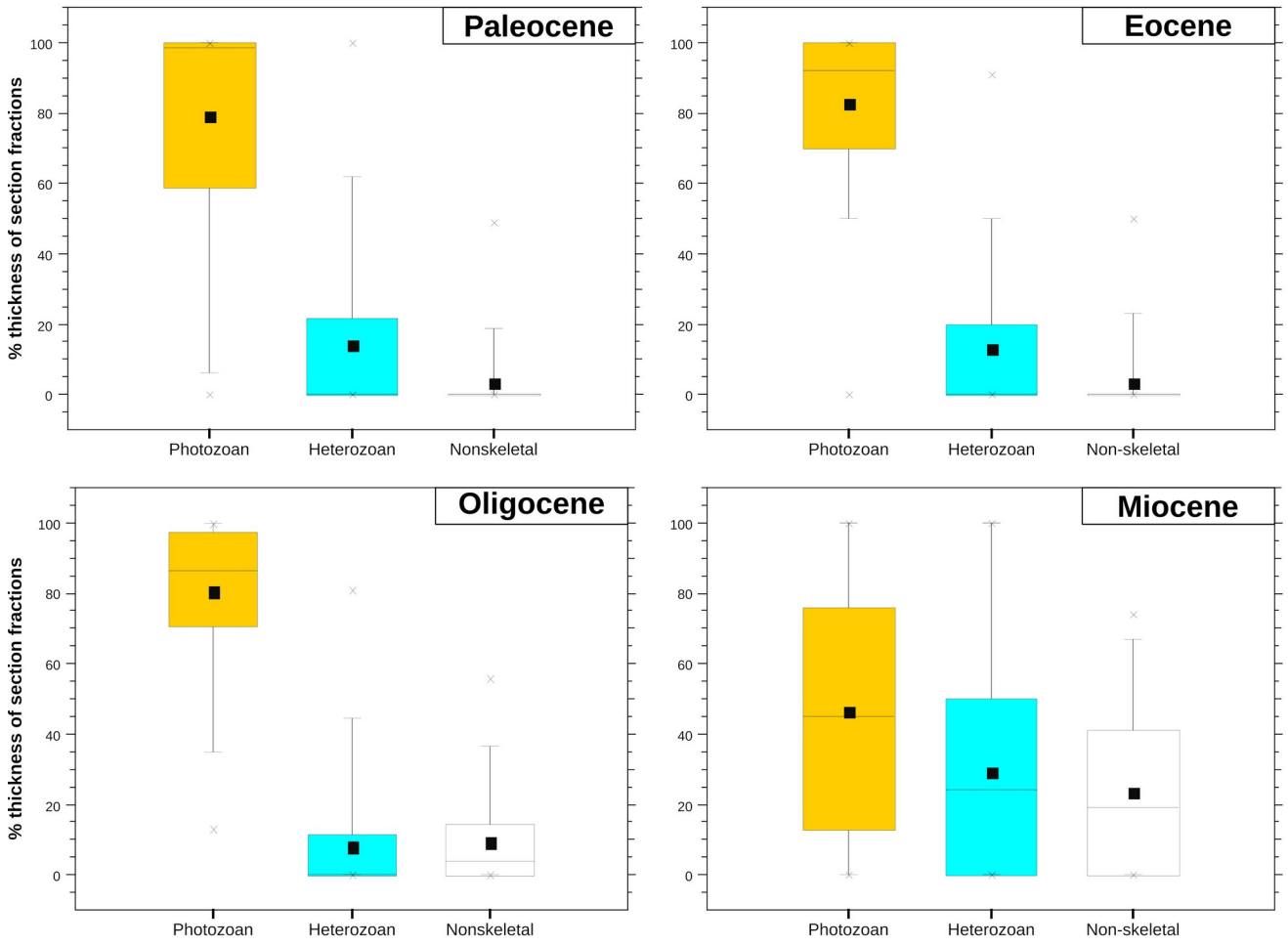

Figure 2: Box and whisker plots showing the Photozoan (yellow), Heterozoan (light blue) and non-skeletal dominated (white) facies distribution in the investigated fossil facies during the different epochs (Paleocene, Eocene, Oligocene, Miocene).

Figure 3: Box and whisker plots showing the distribution during time (Paleocene, Eocene, Oligocene, Miocene) of the LBF dominated and codominated facies (purple), CC dominated and codominated facies (blue), RCA dominated and codominated facies (red), and GCA dominated and codominated facies (green); the key for the statistical symbols of the box and whisker plot is as in Fig. 2.

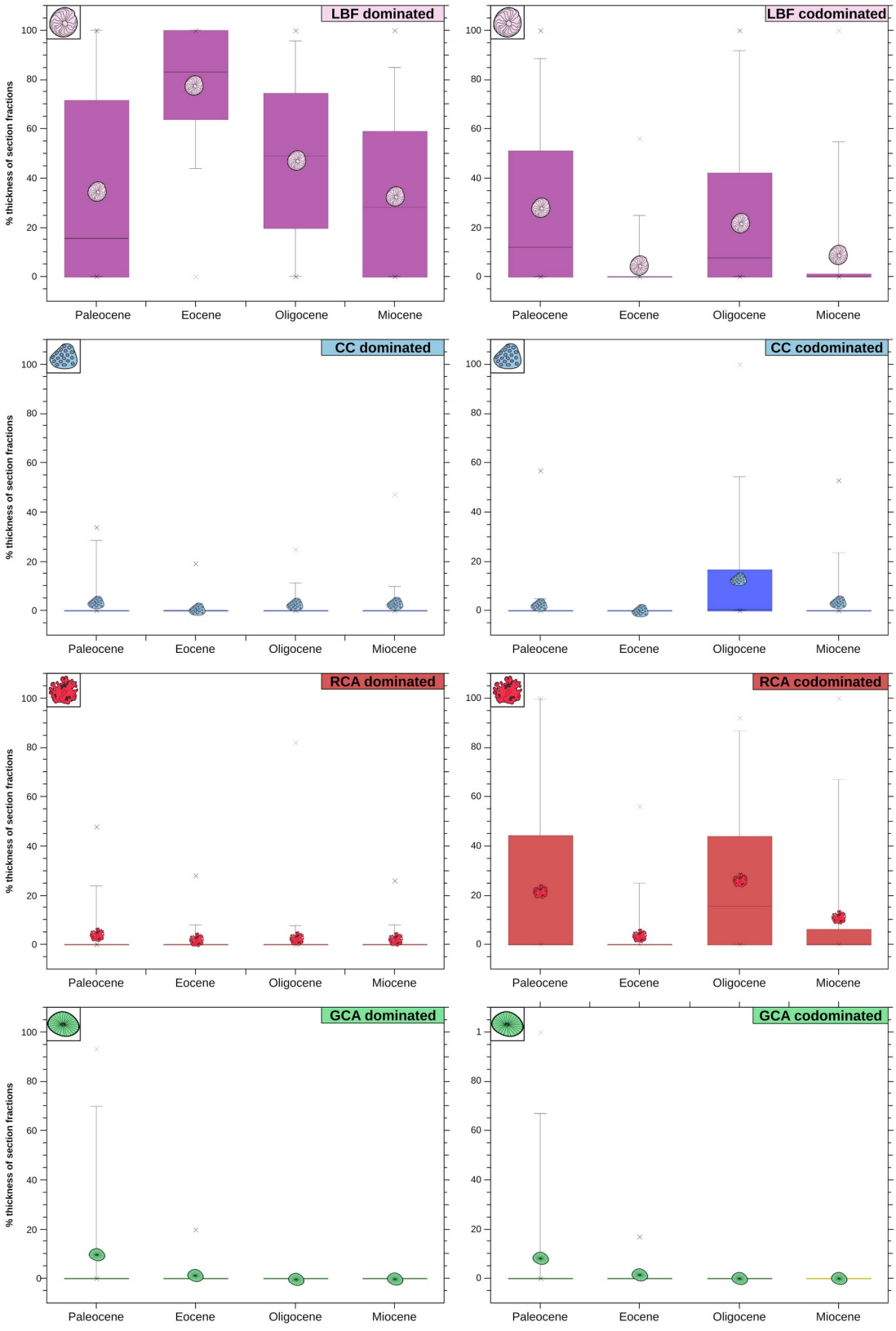
LBF dominated
LBF codominated
CC dominated
CC codominated
RCA dominated
RCA codominated
GCA dominated
GCA codominated
% thickness of section fractions
Paleocene
Eocene
Oligocene
Miocene

Section Average

Dominant components	LBF	LBF & RCA	LBF & GCA	LBF & CC	CC	CC & RCA	CC & EBF	RCA	RCA & Peloids	GCA	GCA & SBF	EBF	SBF	SBF & Peloid	Microbial crusts	Ooids	Peloids	Intraclasts	Mud	Heterozoan
Rupelian	51.35%	22.13%	0.00%	4.35%	2.00%	8.74%	0.00%	1.43%	0.00%	0.00%	0.00%	0.00%	2.17%	0.00%	0.00%	0.00%	1.26%	0.00%	2.82%	3.96%
Chattian	45.50%	15.95%	0.00%	4.73%	1.82%	8.98%	0.00%	2.52%	0.00%	0.00%	0.00%	0.00%	3.41%	0.00%	0.00%	0.45%	1.75%	0.00%	10.84%	4.05%
Aquitanian	30.81%	9.89%	0.00%	0.69%	0.42%	0.47%	0.00%	1.08%	0.00%	0.00%	0.00%	0.00%	11.83%	0.00%	0.08%	11.19%	3.81%	0.00%	20.72%	9.00%
Burdigalian	37.61%	6.95%	0.00%	0.00%	2.45%	1.03%	0.11%	0.87%	0.00%	0.00%	0.00%	0.00%	16.61%	0.00%	0.18%	0.45%	0.84%	0.00%	13.32%	19.61%

Formation Average

Dominant components	LBF	LBF & RCA	LBF & GCA	LBF & CC	CC	CC & RCA	CC & EBF	RCA	RCA & Peloids	GCA	GCA & SBF	EBF	SBF	SBF & Peloid	Microbial crusts	Ooids	Peloids	Intraclast	Mud	Heterozoan
Rupelian	40.20%	15.90%	0.00%	25.00%	1.57%	4.34%	0.00%	1.65%	0.00%	0.00%	0.00%	0.00%	4.53%	0.00%	0.00%	0.00%	0.45%	0.00%	1.90%	4.52%
Chattian	35.28%	14.97%	0.00%	34.67%	1.28%	4.02%	0.00%	2.42%	0.00%	0.00%	0.00%	0.00%	0.83%	0.00%	0.00%	0.10%	0.38%	0.00%	4.41%	1.65%
Aquitanian	15.47%	11.65%	0.00%	5.00%	0.12%	0.14%	0.00%	2.81%	0.00%	0.00%	0.00%	0.00%	7.46%	0.00%	0.02%	10.70%	2.67%	0.00%	11.80%	32.17%
Burdigalian	24.83%	14.41%	0.00%	0.00%	7.56%	0.73%	0.04%	1.35%	0.00%	0.00%	0.00%	0.00%	14.31%	0.00%	0.06%	0.71%	1.11%	0.00%	7.71%	27.19%

Table 4: Percent distribution of the dominant components in the Oligocene (Rupelian, Chattian) and early Miocene (Aquitanian, Burdigalian), following the Section Average and the Formation Average approaches, respectively.

Section Average

Dominated + codominated facies	LBF	CC	RCA	GCA	EBF	Ooids & Peloids	Mud	Microbial crusts	Heterozoan
Paleocene	63.90%	6.07%	25.69%	18.50%	0.00%	3.31%	1.33%	0.24%	14.43%
Eocene	81.70%	0.61%	4.20%	0.72%	2.39%	0.34%	2.95%	0.38%	10.43%
Oligocene	70.24%	14.71%	28.49%	0.00%	0.00%	1.80%	7.81%	0.00%	7.91%
Miocene	42.20%	4.65%	12.33%	0.00%	0.05%	7.58%	15.72%	0.13%	29.00%

Formation Average

Dominated + codominated facies	LBF	CC	RCA	GCA	EBF	Ooids & Peloids	Mud	Microbial crusts	Heterozoan
Paleocene	60.00%	2.36%	26.03%	17.82%	0.00%	2.54%	2.31%	0.26%	13.95%
Eocene	81.61%	0.51%	5.54%	1.83%	2.54%	0.31%	2.04%	0.13%	10.21%
Oligocene	85.95%	36.61%	16.37%	0.00%	0.00%	0.34%	3.19%	0.00%	5.05%
Miocene	29.27%	21.42%	21.22%	0.00%	0.01%	8.59%	5.36%	0.02%	37.63%

Table 3: Percent distribution of the main groups of carbonate grains (dominated plus codominated facies) during Paleocene, Eocene, Oligocene, Miocene, following the Section Average and the Formation Average approaches, respectively.

LBF dominated facies are the most abundant element of the shallow-water carbonates of the study area (Table 2; Fig. 3). Overall, taken together, the facies dominated by LBF and the facies codominated by LBF represent the majority of shallow-water carbonates of the Paleocene, Eocene and Oligocene and Miocene epochs (Table 3; Fig. 4). The abundance of LBF peaks during the Eocene and decreases hereafter. LBF dominated sections (>90% of the section) persist through all periods. Facies dominated solely by RCA are relatively rare, on the other hand, facies codominated by RCA are rather abundant, usually representing the second or third most abundant facies type (generally after LBF dominated and LBF codominated) (Table 2; Fig. 3). RCA codominated facies are relevant during the Paleocene, Oligocene and Miocene and their abundance is the lowest during the Eocene (Table 2; Fig. 3). Taken together CC dominated and CC codominated facies are usually the next most abundant facies type (Table 3; Fig. 4). Their abundance peaks during the Oligocene and has a minimum during the Eocene. GCA facies (either solely considering GCA dominated facies or both GCA dominated and GCA

codominated facies) are only occurring in significant amounts during the Paleocene and Eocene, being more common in the former (Tables 2, 3; Figs. 3, 4). All other producers are uncommon for the entire time period (Paleocene to early Miocene). EBF facies are very rare in all the epochs except in the Eocene where they account for 2.5% of average of section fractions (Tables 2, 3). Microbial crusts-dominated facies are extremely rare during every epoch (Tables 2, 3). Facies characterized by the dominance of non-skeletal grains are relatively rare during the Paleocene and Eocene and become more common during the Oligocene and Miocene (Tables 2, 3; Fig. 2). Intertidal mud dominated facies occur in every epoch and their abundance peaks during the Miocene where they are one of the most common non-skeletal facies type (Tables 2, 3).

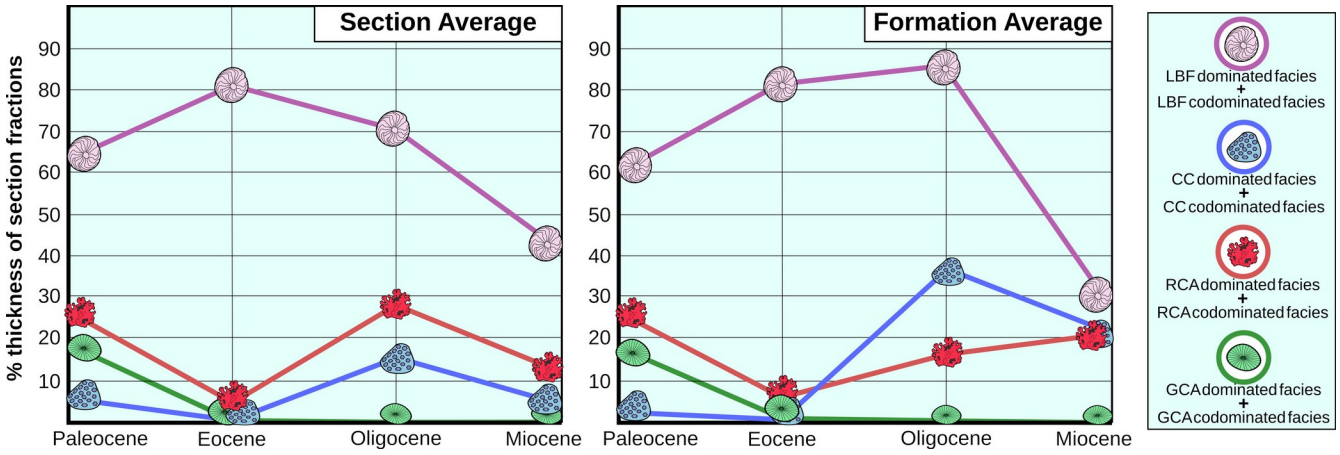

Figure 4: Summary diagrams showing the distribution of the main recognized facies (LBF, CC, RCA, GCA) during the Paleocene, the Eocene, the Oligocene, and the Miocene, using the two different approaches (see Methods): the Section Average and the Formation Average approaches. Note the preponderance of LBF dominated and codominated facies in all the epochs; the key to the symbols of the various carbonate producers is as in Fig. 3; as certain facies can be codominated by, e.g., LBF and CC (and thus be included in both the CC dominated + CC codominated facies and in the LBF dominated + LBF codominated facies), in this graph the total can exceed 100%.

Section Average

Dominant components	LBF	LBF & RCA	LBF & GCA	LBF & CC	CC	CC & RCA	CC & EBF	RCA	RCA & Peloids	GCA	GCA & SBF	EBF	SBF	SBF & Peloid	Microbial crusts	Ooids	Peloids	Intraclasts	Mud	Heterozoan
Paleocene	35.21%	19.40%	9.29%	0.00%	3.38%	2.69%	0.00%	3.60%	0.00%	8.55%	0.67%	0.00%	7.69%	1.81%	0.24%	1.14%	0.36%	0.38%	1.33%	4.26%
Eocene	78.21%	3.21%	0.28%	0.00%	0.61%	0.00%	0.00%	0.95%	0.03%	0.33%	0.11%	2.39%	4.97%	0.00%	0.38%	0.25%	0.07%	0.00%	2.95%	5.35%
Oligocene	47.93%	17.91%	0.00%	4.40%	1.80%	8.51%	0.00%	2.06%	0.00%	0.00%	0.00%	0.00%	2.86%	0.00%	0.00%	0.29%	1.51%	0.00%	7.81%	5.06%
Miocene	33.02%	8.88%	0.00%	0.29%	1.88%	2.42%	0.05%	1.02%	0.00%	0.00%	0.00%	0.00%	13.65%	0.00%	0.13%	4.94%	2.64%	0.00%	15.72%	15.35%

Formation Average

Dominant components	LBF	LBF & RCA	LBF & GCA	LBF & CC	CC	CC & RCA	CC & EBF	RCA	RCA & Peloids	GCA	GCA & SBF	EBF	SBF	SBF & Peloid	Microbial crusts	Ooids	Peloids	Intraclasts	Mud	Heterozoan
Paleocene	35.89%	18.36%	5.74%	0.00%	1.56%	0.81%	0.00%	6.86%	0.00%	11.68%	0.40%	0.00%	7.24%	0.54%	0.26%	1.59%	0.41%	0.57%	2.31%	5.77%
Eocene	77.26%	3.65%	0.71%	0.00%	0.51%	0.00%	0.00%	1.81%	0.08%	0.83%	0.29%	2.54%	6.53%	0.00%	0.13%	0.21%	0.02%	0.00%	2.04%	3.38%
Oligocene	41.34%	11.90%	0.00%	32.71%	0.99%	2.90%	0.00%	1.57%	0.00%	0.00%	0.00%	0.00%	2.82%	0.00%	0.00%	0.05%	0.29%	0.00%	3.19%	2.23%
Miocene	16.36%	9.79%	0.00%	3.13%	7.68%	10.61%	0.01%	0.83%	0.00%	0.00%	0.00%	0.00%	10.51%	0.00%	0.02%	6.74%	1.85%	0.00%	5.36%	27.11%

Table 2: Percent distribution of the dominant components during Paleocene, Eocene, Oligocene, Miocene, following the Section Average and the Formation Average approaches, respectively.

Section Average

Dominated + codominated facies	LBF	CC	RCA	GCA	EBF	Ooids & Peloids	Mud	Microbial crusts	Heterozoan
Rupelian	77.83%	15.09%	32.30%	0.00%	0.00%	1.26%	2.82%	0.00%	6.13%
Chattian	66.18%	15.52%	27.45%	0.00%	0.00%	2.20%	10.84%	0.00%	7.45%
Aquitanian	41.39%	1.58%	11.44%	0.00%	0.00%	15.00%	20.72%	0.08%	20.83%
Burdigalian	44.55%	3.58%	8.84%	0.00%	0.11%	1.29%	13.32%	0.18%	36.21%

Formation Average

Dominated + codominated facies	LBF	CC	RCA	GCA	EBF	Ooids & Peloids	Mud	Microbial crusts	Heterozoan
Rupelian	81.10%	30.91%	21.89%	0.00%	0.00%	0.45%	1.90%	0.00%	9.05%
Chattian	84.92%	39.97%	21.41%	0.00%	0.00%	0.48%	4.41%	0.00%	2.48%
Aquitanian	32.12%	5.26%	14.59%	0.00%	0.00%	13.36%	11.80%	0.02%	39.63%
Burdigalian	39.24%	8.33%	16.49%	0.00%	0.04%	1.81%	7.71%	0.06%	41.49%

Table 5: Percent distribution of the main groups of carbonate grains (dominated plus codominated facies) in the Oligocene (Rupelian, Chattian) and early Miocene (Aquitanian, Burdigalian), following the Section Average and the Formation Average approaches, respectively.

4.2 Rupelian-Burdigalian detailed analysis

Since the Paleocene is mainly represented by Thanetian, the Eocene by the Ypresian, and the Miocene by the early Miocene, the analysis at stage level was performed only in the Rupelian-Burdigalian interval. As in the epoch analysis, the photozoan facies dominate the investigated carbonate successions (Tables 4, 5). The heterozoan facies reach their maximum during the Burdigalian (Tables 4, 5). Both type of calcifiers decrease trough the time period as the non-skeletal grains dominated facies become more significant (Tables 4, 5). LBF dominated facies display a clear peak during the Rupelian and reach their lowest abundance in the Aquitanian (Table 4). By taking together both LBF dominated and LBF codominated facies, the Rupelian peak can no longer be observed in both the formation-average and section-average representations, while the minimum during the Aquitanian still occurs (Table 5). Similarly, the abundance of CC dominated facies (either solely considering CC dominated facies or considering both CC dominated and CC codominated facies)

displays a minimum during the Aquitanian (Tables 4, 5). Both the facies dominated by non-skeletal grains in general and those characterized by intertidal muds specifically peak during the Aquitanian, in both the section-average and in the formation average representations (Tables 4, 5).

5. Discussion

5.1 Carbonate factories evolution

Large benthic foraminifera appear to be the most important carbonate producers within the investigated time-interval in the southern Tethyan realm as they are very common in every region and in every epoch (Tables 2, 3; Figs. 3, 4). They reach their maximum abundance during the Eocene (where they are overwhelmingly dominant) and their lowest during the Miocene (still remaining the most important carbonate producers). Our results indicate that, from the late Paleocene to the early Miocene, in the southern Tethyan realm, the majority share of the biogenic carbonates accumulated in shelfal carbonate factories, has been produced by benthic foraminifera. This now manifest with a large fraction of the shallow water carbonates of the study area being comprised of LBF dominated facies. These results are also supported by the lithostratigraphic information reported by Höntzsch et al. (2011) and Hussein (2019) for Egypt, by Schaub et al. (1995), Buchbinder et al. (2005) and Rosenfeld and Hirsch (2005) for Israel, by Farouk et al. (2013) for Jordan, by Alsharhan and Nairn (1995) for the Arabian Peninsula, by Sadooni and Alsharhan (2019) for UAE, by Bernecker (2014) for Oman, by Sissakian (2013), Ameen-Lawa and Ghafur (2015), and Sadooni and Alsharhan (2019) for Iraq, by Reuter et al. (2009), Van Buchem et al. (2010), Yazdi-Moghadam et al. (2018a), Hadi et al. (2019), Dill et al. (2020) and Benedetti et al. (2021) for Iran, by Akhtar and Butt (1999), Naveed and Chaudhry (2008), Afzal et al. (2010), Özcan et al. (2015), Ahmad et al. (2016), Khan et al. (2018) and Özcan et al. (2018) for Pakistan, by Gaetani et al. (1983), Less et al. (2018) and Sarkar (2018) for India, and by Zhang et al. (2013) for China. Other reviews of carbonate production in the Eurasian province during the Cenozoic also highlighted a remarkable abundance of LBF during the Paleocene, Eocene (where

they dominates), Oligocene and early Miocene (Geel, 2000; Nebelsick et al., 2005; Scheibner and Speijer, 2008; Pomar et al., 2017; Boudagher-Fadel, 2018; Cornacchia et al., 2021). A similar pattern can be also observed in the American province (Aguilera et al., 2020).

In the modern oceans LBF distribution is strongly controlled by temperature (Langer and Hottinger, 2000; Renema et al., 2018) and so is their diversity. Tropical assemblages display a much large number of genera and species than sub-tropical ones (Beavington-Penney and Racey, 2004). During the early Eocene, following an extinction event at the Paleocene-Eocene boundary, LBF became significantly more diverse with the rise of large nummulitids that would dominate LBF assemblage until the Bartonian (Boudagher-Fadel, 2018; Benedetti and Papazzoni, 2022). The high temperatures of the early Eocene as well as the temperature drop at the end of the Bartonian (Zachos et al. 2001), suggests, as already noted by other authors (e.g., Scheibner and Speijer, 2008), a strong relation between temperature and LBF abundance. During the early Paleogene their dominance started at low-latitudes and progressed towards higher latitudes as temperatures rose, paralleled by a decrease of CC (Scheibner and Speijer, 2008; Martín-Martín et al., 2020). Therefore LBF success during the Paleogene would have been favored by the green-house conditions that prevailed for most of the period (except during the Oligocene, when the opening of the Tasmanian and Drake passages lead to the isolation and the progressive build-up of ice on Antartica) (Zachos et al., 2001). Our dataset clearly shows that LBF facies peak in the Eocene (which is mainly represented by the early Eocene in the database). However, taken together, LBF dominated and codominated facies do not diminish much during the Oligocene. The review of Nebelsick et al. (2005), focused on Eocene circumalpine carbonates, also indicates that LBF facies largely dominated during the middle Eocene, far after the Early Eocene Climatic Optimum. This suggests a more complex pattern. According to Pomar et al. (2017) and Hallock and Seddighi (2022), LBF are perfectly suited to deal with extreme oligotrophic conditions associated with periods of reduced thermohaline circulation. This might have played a role in fostering their abundance during the warm periods of the Paleogene. LBF also seems to be better

adapted than CC to water turbidity related to nutrient abundance (Wilson and Vecsei 2005), and to outperform both CC and RCA in environments characterized by high sedimentation rates (Lokier et al., 2009; Coletti et al., 2021b). We have to remember that, although relatively complex, LBF are unicellular organisms, and thus, they are very flexible. Eventhough throughout the geological time certain groups of LBF clearly evolved pursuing a K-strategy compared to other benthic foraminifera (see Hottinger, 1982), their life cycle is still significantly different from that of multicellular organism like RCA and CC. Furthermore, unlike CC and RCA, they are mobile and so they can relocate if they need to. LBF probably took advantage from the reduced competition in shelfal settings caused by the harsh condition created by the Paleocene Eocene Thermal Maximum and the other Paleogene hyperthermals and, thanks to their adaptability, became able to thrive even after the end of the early Paleogene greenhouse. Encrusting benthic foraminifera, similarly to free-living LBF, reach peak abundance during the Eocene (Tables 3, 4). Presently EBF are relatively rare and mainly produce centimeters-sized nodules (e.g., Hottinger, 1983; Bassi et al., 2012). However, during the early and middle Eocene LBF were a relevant group of reef-builders, creating extensive reefs in the Western Tethys (Perrin, 1992, 2009; Rasser, 1994). While modern EBF do not harbor symbionts (Leutenegger, 1984) and usually occur between 40 and 105 m of water-depth (Rasser and Piller 1997; Bassi et al., 2012), Eocene EBF are often associated with shallow-water assemblages typical of the upper part of the photic zone (e.g., they commonly associated with alveolinids) (Rasser, 1994; Tomás et al., 2016; Coletti et al., 2021b). Both evidence indicate that Eocene EBF might have been relatively different from their modern counterparts. More detailed analysis might help understanding if Eocene EBF were symbiont bearing organisms or not, and thus clarifying the environmental reasons of their abundance during the Eocene.

Colonial corals are abundant in the Paleocene, Miocene and they reach a peak during the Oligocene (Tables 2, 3; Figs. 3, 4). They are rare during the Eocene (Tables 2, 3; Figs. 3, 4). This is also supported by the lithostragraphic information provided by Coletti et al. (2021a) for Cyprus, by Kuss

and Boukhary (2008) for Egypt, by Whittle et al. (1995) and Sadooni and Alsharhan (2019) for UAE, by Bernecker (2014) for Oman, by Sissakian (2013), Ameen-Lawa and Ghafur (2015), Ghafur (2015) and Sadooni and Alsharhan (2019) for Iraq, by Reuter et al. (2009), Van Buchem et al. (2010), Ghaedi et al. (2016), Yazdi-Moghadam et al. (2018, 2021) and Dill et al. (2020) for Iran, by Afzal et al. (2010) for Pakistan, by Less et al. (2018) and Sarkar (2018) for India. Our results are overall consistent with other reviews of CC distribution in the Eurasian province (Perrin and Bosellini, 2012; Scheibner and Speijer, 2008; Pomar et al., 2017), East Pacific province (López-Pérez, 2005, 2017) and American province (Budd, 2000; Johnson et al., 2008), that indicate the Oligocene as a favorable period for both CC and CC dominated reefs.

Similarly to LBF, this pattern seems to be strongly connected to global temperatures. During the Paleocene, in the Eurasian province, CC are actually more abundant during the early to late Paleocene (Scheibner and Speijer, 2008; Martín-Martín et al., 2020). This time-interval is characterized by temperatures lower than those of the latest Paleocene and the following early Eocene (Barnett et al. 2019). During the Eocene, in the Eurasian province, CC are relatively rare and became relevant carbonate producers only during the late Eocene (Nebelsick et al. 2005; Scheibner and Speijer, 2008; Bernecker, 2014), which is the coldest stage of the epoch (Zachos et al., 2001). The Oligocene is the coldest period of the Paleogene (Zachos et al., 2001), and it is recognized worldwide as a period of great abundance of CC (Dishon et al., 2020). During the early Miocene CC are still very common, but during the middle Miocene, worldwide, RCA become significantly more abundant in tropical shelf at the expenses of CC (Esteban, 1979, 1996; Halfar and Mutti, 2005; López-Pérez, 2005; Cornacchia et al., 2021; Bialik et al., 2022). CC abundance increases again in the late Miocene in the Western Tethys (Esteban, 1979, 1996; Pomar and Hallock, 2007; Pomar et al., 2017; Cornacchia et al., 2021) and in the Plio-Pleistocene in the East Pacific and in the Caribbean (López-Pérez, 2005; Johnson et al., 2008). Thus, the distribution of CC during the Neogene can be also related to temperatures. CC are less abundant in the warm Middle Miocene Climatic Optimum and more abundant during cooler periods

(Zachos et al., 2001; Herbert et al., 2016; Steinthorsdottir et al., 2020; Dishon et al., 2020). As CC presently thrive in a narrow temperature range and are severely damaged (i.e., the coral bleaching) whenever temperatures exceed this threshold (e.g., Marshall and Clode, 2004; Crabbe, 2008), it is conceivable that the warm peaks of the Cenozoic might had a detrimental effect on CC abundance. Colder periods are also characterized by a stronger oceanic circulation than warmer periods, and this factor could also have favored CC over other carbonate producers like LBF (e.g., Pomar et al., 2017). Furthermore, colder periods are favorable towards aragonite-producing organisms like CC (e.g., Hallock, 1997; Scheibner and Speijer, 2008), whereas the ocean chemistry of warm periods (like the Paleocene-Eocene) is favorable to calcite generation (Stanley, 2006) and possibly detrimental to CC. However, we must also consider that the low pH (Boudreau et al., 2019), which characterized most of the Paleocene and Eocene, likely had a significant negative impact also on the accumulation and preservation potential of CC – if they even calcified in shallow water at this time and had not shifted to a non-calcificing lifestyle (Fine and Tchernov 2007). With the currently available data, disentangling the effects of these factors is probably impossible, although it is clear that temperature played an important role.

RCA abundance displays a pattern similar to the one of CC and characterized by a minimum during the Eocene (Tables 2, 3; Figs. 3, 4). This is supported by the lithostratigraphic information provided by Coletti et al. (2021) for Cyprus, by Kuss and Boukhary (2008) for Egypt, by Whittle et al. (1995) for UAE, by Afzal et al. (2010) for Pakistan, by Bernecker (2014) for Oman, by Seyrafian and Toraby (2005), Reuter et al. (2009), Ghaedi et al. (2016) and Yazdi-Moghadam et al. (2021) for Iran. Within the various sections the abundance of CC and RCA codominant facies shows a positive correlation in the Paleocene and in the Miocene, but not as clearly during the Eocene and the Oligocene (Fig. 3).

Modern RCA are extremely adaptable and can thrive in both warm and cold climates, in both oligotrophic and nutrient-rich water and from the shallow intertidal zone to the lowest limit of the

photic zone (e.g., Riosmena-Rodríguez, 2017; Pomar et al., 2017). CC requires a hard substrate for their initial recruitment on the seafloor and RCA can generate hard-substrates. Free-living nodules can progressively coalesce leading to the creation of a hard substrate suitable for the colonization of other organisms or the expansion of RCA bioconstructions. In turn the complex framework of CC-reefs creates several niches that can be used by coralline algae. Therefore, to a certain extent, the two groups are mutually beneficial to one another, justifying why the periods favorable for the former can be also favorable for the latter. However, we also need to consider that most of the analyzed papers pay little attention to RCA in comparison to LBF (which are useful for biostratigraphy), and CC (that can be easily observed in the outcrops), therefore a bias in the database that could lead to an underestimation of RCA can not be excluded.

Within the study area, in the Paleocene, GCA are rarely a dominant component of the skeletal assemblage (Tables 2, 3; Figs. 3, 4). In the Eocene they dominate very rarely, while in the Oligocene and in the Miocene they occur only as a minor component of the skeletal assemblage. These results are supported by the lithostragratiphic information provided by Höntzsch et al. (2011) for Egypt, by Nafarieh et al. (2019) and Benedetti et al. (2020) for Iran, by Akhtar and Butt (1999), Afzal et al. (2010), Khan et al. (2018) and Khitab et al. (2020) for Pakistan, by Gaetani et al. (1983) for India, and by Zhang et al. (2013) for China. Differently from our results, the review of Pomar et al. (2017) of Cenozoic carbonates of western-central Tethys indicates abundant GCA only in the Danian (mainly dasyclads) and in the Miocene (mainly Halimedales). Based on the fossil record, during the Cenozoic, GCA biodiversity peaks in the Paleocene and decreases afterwards (Aguirre and Riding, 2005). This pattern is consistent with the abundance of GCA in the successions of the study area. However, while biodiversity may be related to abundance it is usually decoupled from carbonate production (e.g., Johnson et al. 2008). Modern GCA mostly precipitate aragonite and are thus easily susceptible to diagenetic dissolution, which can start even when the alga is still alive (Granier, 2012). Several fossil taxa of Dasycladales are thought to have precipitate calcite instead of aragonite (Granier, 2012). The

last of these supposedly calcitic taxa occurred during the Eocene (Granier, 2012). Therefore, the observed pattern of GCA distribution might be, possibly in a similar to CC, related to a preservation bias as opposed to an environmental variable like in the case of LBF. The progressive decrease of GCA abundance throughout the Cenozoic in this region might have been connected to a transition from early Paleogene assemblages rich of calcite-producing taxa to Neogene assemblage entirely constituted of aragonitic taxa.

5.2 Regional and global implications

Several remarkable similarities can be observed by comparing our results for the Southwestern and Western Central Asia with the other few available reviews of carbonate production: the peak in LBF abundance during the Eocene and the increase in coral abundance during the Oligocene (Kiessling et a., 1999; Nebelsick et al., 2005; Johnson et al., 2008; Scheibner and Speijer, 2008; Pomar et al., 2017; Aguilera et al., 2020). These changes are likely to have been strongly related to temperature, as the global increase in both CC diversity and importance as carbonate producers, is paired with a decrease in temperatures, while the Eocene widespread abundance of LBF is heralded by high global temperatures (Zachos et a., 2001). CC achieve the highest calcification rates within a narrow temperature range (e.g., Marshall and Clode, 2004; Crabbe, 2008). This range is usually much larger for LBF (e.g., Titelboim et al. 2019), suggesting that LBF can take advantage of the detrimental effect that very high-temperatures have on their competitors. Our dataset is backed by a quantitative data on facies abundance, and thus provide a strong argument in favor of the major rearrangements of shallow water carbonate factories at the Paleocene-Eocene and Eocene-Oligocene boundaries indicated by the other reviews. As these changes are witnessed at the global scale and are most likely temperature-driven, they provide a clear evidence on the long term effect of temperatures on carbonate factories and shelfal biomes.

Differently from the northwestern Mediterranean Tethys area analyzed by (Pomar and Hallock, 2007; Pomar et al., 2004, 2012, 2017), LBF are always the dominant carbonate producers, even after the Eocene. LBF in northwestern Mediterranean Tethys are reported to diminish during the Oligocene and show a resurgence during the Miocene (Pomar et al., 2017). This is not observed in our study area. Such a difference could be still, at least partially, temperature related, as our study area was located southern than the northwestern Mediterranean Tethys and thus was probably more favorable for LBF. During the Oligocene and the early Miocene, thanks to global cooling and a progressive north-ward shift, the southern Tethys became more favorable to CC, leading to their increase. This cooling is also testified by the progressive increase of Heterozoan carbonate facies (Fig. 2). While in the northwestern Mediterranean Tethys RCA abundance increases only in the Miocene, in the study area, RCA dominated facies become very common already in the Oligocene following the increase in CC, suggesting a favorable relationship with the two groups.

The abundance of non-skeletal facies related to restricted conditions (Flugel, 2004) peaks in the early Miocene and in particular in the Aquitanian. This is also supported by the lithostratigraphic information provided by Al-Juboury and McCann (2008) and Ameen-Lawa and Ghafur (2015) for Iraq, Reuter et al. (2009) and Mohammadi et al. (2013) for Iran. During the Miocene the convergence between the African-Arabian and Eurasian plate lead to the progressive restriction and then to the closure of the Mediterranean-Indian Ocean Seaway (e.g., Rogl et al., 1998; Robertson et al., 2012). Sedimentation rates in the Eastern Mediterranean indicates that most of the deep water restriction occurred in the 24 - 21 Ma interval (Torfstein and Steinberg, 2020), while Nd isotopes indicates that surface water exchange was reduced by ~90% at ca. 20 Ma (Bialik et al., 2019). Consequently, although a shallow connection between the two basins persisted for much longer (e.g., Buchbinder, 1996; Sissakian, 2013; Cornacchia et al., 2018), most of the restriction occurred during the Aquitanian, consistently with the observed peak of carbonate facies related to restricted marine conditions.

6. Conclusions

The quantitative analysis of facies distribution in the Paleocene to Miocene outcrops of shallow water carbonates of the Southwestern and Western Central Asia highlighted several trends in the composition of carbonate factories and in the abundance of carbonate producing organisms. Large benthic foraminifera resulted the most important group of carbonate producers during the whole investigated period, with their importance peaking during the Eocene and dwindling only during the Miocene. The abundance of colonial corals is the highest during the Oligocene and the lowest during the Eocene (which in the database is mainly represented by the lower Eocene). Both patterns seem to related to global temperatures which (within the investigated time-period) reach their maximum during the early Eocene and their lowest in Oligocene. Colonial corals achieve the highest calcification rate in a very narrow temperature range compared to large benthic foraminifera. The very high temperatures of the early Paleogene, in the tropical ocean that was the southern Tethys, might, thus, have favored large benthic foraminifera dominated carbonate factories. Thanks to their adaptability large benthic foraminifera would have kept their position as dominant carbonate producers for the whole period, even after the end of the early Paleogene green-house. Red calcareous algae display a patter much like the one of colonial corals. Since red calcareous algae and colonial corals are currently the main framework builder of shallow-water tropical reefs it is possible that, on the large scale, the two groups are probably mutually beneficial to one another in terms of carbonate production. Green calcareous algae decrease from the Paleocene onward. As the last taxa of presumably calcitic green calcareous algae went extinct during the Eocene, it is possible that their overall decrease as carbonate producers might be related to a preservation bias connected to the transition toward modern assemblages that are entirely constituted by fragile, aragonite-producing, taxa.

Nutrient abundance and seawater chemistry most likely also played a role in shaping these large-scale patterns of carbonate production. However, any attempt at disentangling the weight of the

various variables not backed by more accurate and standardized data on the skeletal assemblages, would be only speculative.

The Aquitanian peak in the abundance of carbonate facies related to very shallow and/or restricted marine conditions is most likely connected to the progressive narrowing of the Tethys related to the ongoing collision with the Arabian plate.

Overall, this analysis displays a clear agreement between large-scale patterns in shallow-water carbonate sedimentation and both environmental and geological processes, indicating the trove of information locked within the shallow-water sedimentary record. However, to unlock this potential, a standardized, quantitative and reproducible approach is absolutely necessary.

Acknowledgments

G.C., L.M., and G.B. would like to thank Milano Bicocca University for funding their doctoral and post-doctoral grants. O.M.B. is supported by Marie Skłodowska Curie fellowship (101003394-RhodoMalta). The first and last authors are also grateful to IAS for supporting their research activities and for creating an environment conducive to the development of this study. This research represents a scientific contribution of Project MIUR - Dipartimenti di Eccellenza 2018-2022.

Supplementary Material:

Supplementary Table 1. Complete database, including all the facies recognized in the source material, their thickness and their new classification; the database is also accessible online https://doi.org/10.6084/m9.figshare.19323821.v1

References

Adabi, M. H., Kakemem, U. and Sadeghi, A. (2016) Sedimentary facies, depositional environment, and sequence stratigraphy of Oligocene–Miocene shallow water carbonate from the Rig Mountain, Zagros basin (SW Iran). Carbonates and evaporites, 31(1), 69-85.

Adabi, M. H., Zohdi, A., Ghabeishavi, A. and Amiri-Bakhtiyar, H. (2008) Applications of nummulitids and other larger benthic foraminifera in depositional environment and sequence stratigraphy: an example from the Eocene deposits in Zagros Basin, SW Iran. Facies, 54(4), 499-512.

Afzal, J., Williams, M. and Aldridge, R. J. (2009) Revised stratigraphy of the lower Cenozoic succession of the Greater Indus Basin in Pakistan. Journal of Micropalaeontology, 28(1), 7-23.

Afzal, J., Williams, M., Leng, M. J. and Aldridge, R. J. (2011) Dynamic response of the shallow marine benthic ecosystem to regional and pan-Tethyan environmental change at the Paleocene–Eocene boundary. Palaeogeography, Palaeoclimatology, Palaeoecology, 309(3-4), 141-160.

Afzal, J., Williams, M., Leng, M. J., Aldridge, R. J. and Stephenson, M. H. (2011) Evolution of Paleocene to Early Eocene larger benthic foraminifer assemblages of the Indus Basin, Pakistan. Lethaia, 44(3), 299-320.

Agard, P., Omrani, J., Jolivet, L., Whitechurch, H., Vrielynck, B., Spakman, W., Monié P., Meyer B. and Wortel, R. (2011) Zagros orogeny: a subduction-dominated process. Geological Magazine, 148(5-6), 692-725.

Aguilera, O., Bencomo, K., de Araújo, O.M.O., Dias, B.B., Coletti, G., Lima, D., Silane, A.F., Polk, M., Alves-Martin, M.V., Jaramillo, C., Kutter, V.T. and Lopes, R.T., (2020) Miocene heterozoan carbonate systems from the western Atlantic equatorial margin in South America: The Pirabas Formation. Sedimentary Geology, 407, 1–28. https://doi.org/10.1016/j.sedgeo.2020.105739.

Aguirre, J., Riding, R. and Braga, J. C. (2000) Diversity of coralline red algae: origination and extinction patterns from the Early Cretaceous to the Pleistocene. Paleobiology, 26(4), 651-667.

Aguirre, J. and Riding, R. (2005) Dasycladalean algal biodiversity compared with global variations in temperature and sea level over the past 350 Myr. Palaios, 20(6), 581-588.

Ahmad, S., Kroon, D., Rigby, S. and Khan, S. (2016) Paleogene Nummulitid biostratigraphy of the Kohat and Potwar Basins in north-western Pakistan with implications for the timing of the closure of eastern Tethys and uplift of the western Himalayas. Stratigraphy, 13, 277-301.

Ahmad, S., Wadood, B., Khan, S., Ullah, A., Mustafa, G., Hanif, M. and Ullah, H. (2020) The sedimentological and stratigraphical analysis of the Paleocene to Early Eocene Dungan Formation, Kirthar Fold and Thrust Belt, Pakistan: implications for reservoir potential. Journal of Sedimentary Environments, 5(4), 473-492.

Akhtar, M. and Butt, A. A. (1999) Microfacies and foraminiferal assemblages from the early Tertiary rocks of the Kala Chitta Range (Northern Pakistan). Géologie Méditerranéenne, 26(3), 185-201.

Al-Juboury, A. I. and McCann, T. (2008) The Middle Miocene Fatha (Lower Fars) Formation, Iraq. GeoArabia, 13(3), 141-174.

Al-Kahtany, K. M. (2017) Facies development of the Middle Miocene reefal limestone in northwest Saudi Arabia. Journal of African Earth Sciences, 130, 134-140.

Al-Qayim, B., Ibrahim, A. and Kharajiany, S. (2016) Microfacis and sequence stratigraphy of the Oligocene–Miocene sequence at Golan Mountian, Kurdistan, Iraq. Carbonates and Evaporites, 31(3), 259-276.

Alsharhan, A. S. and Nairn, A. E. M. (1995) Tertiary of the Arabian Gulf: sedimentology and hydrocarbon potential. Palaeogeography, Palaeoclimatology, Palaeoecology, 114(2-4), 369-384.

Ameen-Lawa, F. A. and Ghafur, A. A. (2015) Sequence stratigraphy and biostratigraphy of the prolific late Eocene, Oligocene and early Miocene carbonates from Zagros fold-thrust belt in Kurdistan region. Arabian Journal of Geosciences, 8(10), 8143-8174.

Amirshahkarami, M. (2013) Microfacies correlation analysis of the Oligocene-Miocene Asmari Formation, in the central part of the Rag-e-Safid anticlinal oil field, Zagros Basin, south-west Iran. Turkish Journal of Earth Sciences, 22(2), 204-219.

Amirshahkarami, M. and Karavan, M. (2015) Microfacies models and sequence stratigraphic architecture of the Oligocene–Miocene Qom Formation, south of Qom City, Iran. Geoscience Frontiers, 6(4), 593-604.

Amirshahkarami, M., Vaziri-Moghaddam, H. and Taheri, A. (2007) Paleoenvironmental model and sequence stratigraphy of the Asmari Formation in southwest Iran. Historical Biology, 19(2), 173-183.

Amirshahkarami, M., Vaziri-Moghaddam, H. and Taheri, A. (2007) Sedimentary facies and sequence stratigraphy of the Asmari Formation at chaman-Bolbol, Zagros Basin, Iran. Journal of Asian Earth Sciences, 29(5-6), 947-959.

Amirshahkarami, M. and Zebarjadi, E. (2018) Late Paleocene to Early Eocene larger benthic foraminifera biozones and microfacies in Estahbanate area, Southwest of Iran with Thetyan biozones correlation. Carbonates and Evaporites, 33(4), 869-884.

An, W., Hu, X., Garzanti, E., Wang, J. G., and Liu, Q. (2021) New precise dating of the India-Asia collision in the Tibetan Himalaya at 61 Ma. Geophysical Research Letters, 48(3), e2020GL090641.

Avarjani, S., Mahboubi, A., Moussavi-Harami, R., Amiri-Bakhtiar, H. and Brenner, R. L. (2015) Facies, depositional sequences, and biostratigraphy of the Oligo-Miocene Asmari Formation in Marun oilfield, North Dezful Embayment, Zagros Basin, SW Iran. Palaeoworld, 24(3), 336-358.

Avni, Y., Segev, A. and Ginat, H. (2012) Oligocene regional denudation of the northern Afar dome: Pre-and syn-breakup stages of the Afro-Arabian plate. Bulletin, 124(11-12), 1871-1897.

Babazadeh, S. A. and Alavi, M. (2013) Paleoenvironmental model for Early Eocene larger benthic foraminiferal deposits from south Birjand region, east Iran. Revue de Paléobiologie, Genève, 32(1), 223-233.

Barnet, J. S., Littler, K., Westerhold, T., Kroon, D., Leng, M. J., Bailey, I., Röhl, U. and Zachos, J. C. (2019) A high-Fidelity benthic stable isotope record of late Cretaceous–early Eocene climate change and carbon-cycling. Paleoceanography and Paleoclimatology, 34(4), 672-691.

Bagherpour, B. and Vaziri, M. R. (2012) Facies, paleoenvironment, carbonate platform and facies changes across Paleocene Eocene of the Taleh Zang Formation in the Zagros Basin, SW-Iran. Historical Biology, 24(2), 121-142.

Ballato, P., Mulch, A., Landgraf, A., Strecker, M. R., Dalconi, M. C., Friedrich, A. and Tabatabaei, S. H. (2010) Middle to late Miocene Middle Eastern climate from stable oxygen and carbon isotope data, southern Alborz mountains, N Iran. Earth and planetary science letters, 300(1-2), 125-138.

Banerjee, S., Khanolkar, S. and Saraswati, P. K. (2018) Facies and depositional settings of the Middle Eocene-Oligocene carbonates in Kutch. Geodinamica acta, 30(1), 119-136.

Bassi, D., Iryu, Y., Humblet, M., Matsuda, H., Machiyama, H., Sasaki, K., Matsuda S., Arai, K. and Inoue, T. (2012) Recent macroids on the Kikai jima shelf, Central Ryukyu Islands, Japan. Sedimentology, 59, 2024-2041.

Basso, D., Coletti, G., Bracchi, V. A. and Yazdi-Moghadam, M. (2019) Lower oligocene coralline algae of the Uromieh section (Qom Formation, NW Iran) and the oldest record of Titanoderma pustulatum (Corallinophycidae, Rhodophyta). Rivista Italiana di Paleontologia e Stratigrafia, 125(1).

Beavington-Penney, S. J. and Racey, A. (2004) Ecology of extant nummulitids and other larger benthic foraminifera: applications in palaeoenvironmental analysis. Earth-Science Reviews, 67(3-4), 219-265.

Beavington-Penney, S. J., Wright, V. P. and Racey, A. (2006) The middle Eocene Seeb Formation of Oman: an investigation of acyclicity, stratigraphic completeness, and accumulation rates in shallow marine carbonate settings. Journal of Sedimentary Research, 76(10), 1137-1161.

Benedetti, A., Consorti, L., Schlagintweit, F. and Rashidi, K. (2021) *Ornatorotalia* pila n. sp. from the late Palaeocene of Iran: ecological, evolutionary and paleobiogeographic inferences. Historical Biology, 33(9), 1796-1803.

Benedetti, A., Papazzoni, A. (2022) Rise and fall of rotaliid foraminifera across the Paleocene and Eocene times. Micropaleontology, 68, 185-196.

Bernecker, M. (2014) Palaeogene carbonates of Oman: lithofacies and stratigraphy. In STRATI 2013 (pp. 71-74). Springer, Cham.

Bialik, O. M., Frank, M., Betzler, C., Zammit, R. and Waldmann, N. D. (2019) Two-step closure of the Miocene Indian Ocean Gateway to the Mediterranean. Scientific Reports, 9(1), 1-10.

Bialik, O. M., Reolid, J., Kulhanek, D. K., Hincke, C., Waldmann, N. D. and Betzler, C. (2022) Sedimentary response to current and nutrient regime rearrangement in the Eastern Mediterranean during the early to middle Miocene (Southwestern Cyprus). Palaeogeography, Palaeoclimatology, Palaeoecology, 588, 110819.

Blondeau A., Bassoulet J.P., Colchen M., Han T.L., Marcoux J., Mascle G. and Van Haver T. (1986) Disparition des formations marines à l'Éocène inférieur en Hymalaia. Sciences de la Terre, Memorire, 47, 103-111.

Bosellini, F. and Perrin, C. (2008) Estimating Mediterranean Oligocene-Miocene Sea surface temperatures: an approach based on coral taxonomic richness. Palaeogeogr. Palaeoclimatol. Palaeoecol. 258, 71–88.

BouDagher-Fadel, M.K., (2018) Evolution and geological significance of larger benthic foraminifera. University College London Press, London, 693 pp.

Boudreau, B. P., Middelburg, J. J., Sluijs, A. and van der Ploeg, R. (2019) Secular variations in the carbonate chemistry of the oceans over the Cenozoic. Earth and Planetary Science Letters, 512, 194-206.

Buchbinder, B. (1996) Miocene carbonates of the Eastern Mediterranean, the Red Sea and the Mesopotamian Basin: geodynamic and eustatic controls, in: Franseen, E.K., Esteban, M., Ward, W.C., Rouchy, J.M., (Eds.), Models for carbonate stratigraphy, from Miocene reef complex of the Mediterranean area. Concepts in Sedimentology and Paleontology 5, Society for Sedimentary Geology, Tulsa, Oklaoma, U.S.A. pp. 89-96.

Buchbinder, B., Calvo, R. and Siman-Tov, R. (2005) The Oligocene in Israel: A marine realm with intermittent denudation accompanied by mass-flow deposition. Israel Journal of Earth Sciences, 54(2).

Budd, A. F. (2000) Diversity and extinction in the Cenozoic history of Caribbean reefs. Coral Reefs, 19(1), 25-35.

Coletti, G., Basso, D., Betzler, C., Robertson, A. H., Bosio, G., El Kateb, A., Foubert, A., Meilijson, A. and Spezzaferri, S. (2019) Environmental evolution and geological significance of the Miocene carbonates of the Eratosthenes Seamount (ODP Leg 160). Palaeogeography, Palaeoclimatology, Palaeoecology, 530, 217-235.

Coletti, G., Basso, D. and Frixa, A. (2017) Economic importance of coralline carbonates. In Rhodolith/Maërl Beds: A Global Perspective (pp. 87-101). Springer, Cham.

Coletti, G., Balmer, E.M., Bialik, O.M., Cannings, T., Kroon, D., Robertson, A.H.F. and Basso, D. (2021) a. Microfacies evidence for the evolution of Miocene coral-reef environments in Cyprus. Palaeogeogr. Palaeoclimatol. Palaeoecol. 11067.

Coletti, G., Mariani, L., Garzanti, E., Consani, S., Bosio, G., Vezzoli, G., Xiumian, H. and Basso, D. (2021) b. Skeletal assemblages and terrigenous input in the Eocene carbonate systems of the Nummulitic Limestone (NW Europe). Sedimentary Geology, 425, 106005.

Corlett, H. J., Bastesen, E., Gawthorpe, R. L., Hirani, J., Hodgetts, D., Hollis, C. and Rotevatn, A. (2018) Origin, dimensions, and distribution of remobilized carbonate deposits in a tectonically active zone, Eocene Thebes Formation, Sinai, Egypt. Sedimentary Geology, 372, 44-63.

Cornacchia, I., Agostini, S. and Brandano, M. (2018) Miocene oceanographic evolution based on the Sr and Nd isotope record of the Central Mediterranean. Paleoceanography and Paleoclimatology, 33(1), 31-47.

Cornacchia, I., Brandano, M. and Agostini, S. (2021) Miocene paleoceanographic evolution of the Mediterranean area and carbonate production changes: A review. Earth-Science Reviews, 221, 103785.

Crabbe, M. J. C. (2008) Climate change, global warming and coral reefs: Modelling the effects of temperature. Computational Biology and Chemistry, 32(5), 311-314.

Daraei, M., Amini, A. and Ansari, M. (2015) Facies analysis and depositional environment study of the mixed carbonate–evaporite Asmari Formation (Oligo-Miocene) in the sequence stratigraphic framework, NW Zagros, Iran. Carbonates and evaporites, 30(3), 253-272.

Dercourt, J., Gaetani, M., Vrielynk, B., Barrier, E., Biju-Duval, B., Brunet, M.F., Cadet, J.P, Crasquin, S. and Sandulescu, M., (2000) Atlas Peri-Tethys, Palaeogeographical Maps.

Dill, M. A., Seyrafian, A. and Vaziri-Moghaddam, H. (2012) Palaeoecology of the Oligocene-Miocene Asmari Formation in the Dill Anticline (Zagros Basin, Iran). Neues Jahrbuch für Geologie und Paläontologie-Abhandlungen, 167-184.

Dill, M. A., Vaziri-Moghaddam, H., Seyrafian, A. and Behdad, A. (2018) Oligo-Miocene carbonate platform evolution in the northern margin of the Asmari intra-shelf basin, SW Iran. Marine and Petroleum Geology, 92, 437-461.

Dill, M. A., Vaziri-Moghaddam, H., Seyrafian, A., Behdad, A. and Shabafrooz, R. (2020) A review of the Oligo–Miocene larger benthic foraminifera in the Zagros basin, Iran; New insights into biozonation and palaeogeographical maps. Revue de Micropaléontologie, 66, 100408.

Dishon, G., Grossowicz, M., Krom, M., Guy, G., Gruber, D. F. and Tchernov, D. (2020) Evolutionary traits that enable scleractinian corals to survive mass extinction events. Scientific Reports, 10(1), 1-10.

Esteban, M. (1979) Significance of the upper Miocene coral reefs of the western Mediterranean. Palaeogeography Palaeoclimatology Palaeoecology, 29, 169-188.

Esteban, M. (1996) An overview of of Miocene reefs from Mediterranean areas: general trends and facies models, In: Franseen, E.K., Esteban, M., Ward, W.C., Rouchy, J.M. (eds.), Models for Carbonate Stratigraphy, from Miocene Reef Complex of the Mediterranean Area. Concepts in Sedimentology and Paleontology 5, Society for Sedimentary Geology, Tulsa, Oklaoma, U.S.A. pp. 3-53.

Fahad, M., Khan, M. A., Hussain, J., Ahmed, A. and Yar, M. (2021) Microfacies analysis, depositional settings and reservoir investigation of Early Eocene Chorgali Formation exposed at Eastern Salt Range, Upper Indus Basin, Pakistan. Carbonates and Evaporites, 36(3), 1-18.

Farouk, S., Ahmad, F. and Smadi, A. A. (2013) Stratigraphy of the Middle Eocene–Lower Oligocene successions in northwestern and eastern Jordan. Journal of Asian Earth Sciences, 73, 396-408.

Fine, M. and Tchernov, D. (2007) Scleractinian coral species survive and recover from decalcification. Science, 315(5820), 1811-1811.

Flügel, E. (2004) Microfacies of Carbonate Rocks. Springer, Berlin, Heidelberg.

Gaetani, M., Nicora, A., Premoli-Silva, I., Fois, E., Garzanti, E. and Tintori, A. (1983) Upper Cretaceous and Paleocene in Zanskar Range (NW Himalaya). Rivista Italiana di Paleontologia e Stratigrafia, 89, 81-118.

Garzanti, E., Al-Juboury, A.I., Zoleikhaei, Y., Vermeesch, P., Jotheri, J., Akkoca, D.B., Allen, M., Andò, S., Limonta, M., Padoan, M., Resentini, A., Rittner, M., Vezzoli, G., (2016) The Euphrates-Tigris-Karun river system: provenance, recycling and dispersal of quartz-poor foreland-basin sediments in arid climate. Earth Sci. Rev. 162, 107–128.

Geel, T. (2000) Recognition of stratigraphic sequences in carbonate platform and slope deposits: empirical models based on microfacies analysis of Palaeogene deposits in southeastern Spain. Palaeogeography, Palaeoclimatology, Palaeoecology, 155(3-4), 211-238.

Ghaedi, M., Johnson, K. and Yazdi, M. (2016) Paleoenvironmental conditions of Early Miocene corals, western Makran, Iran. Arabian Journal of Geosciences, 9(17), 1-20.

Ghafur, A. A. (2015) Integrated depositional model of the carbonate Kirkuk Group of southern Kurdistan-Iraq. J. Nat. Sci. Res., 5, 79-106.

Ghazi, S., Sharif, S., Zafar, T., Riaz, M., Haider, R. and Hanif, T. (2020) Sedimentology and Stratigraphic Evolution of the Early Eocene Nammal Formation, Salt Range, Pakistan. Stratigraphy and Geological Correlation, 28(7), 745-764.

GholamiZadeh, P., Hu, X., Garzanti, E., and Adabi, M.H. (2021) Constraining the timing of Arabia-Eurasia collision in the Zagros orogen by sandstone provenance (Neyriz, Iran). GSA Bulletin, https://doi.org/10.1130/B35950

Granier, B. (2012) The contribution of calcareous green algae to the production of limestones: a review. Geodiversitas, 34(1), 35-60.

Hadi, M., Less, G. and Vahidinia, M. (2019) Eocene larger benthic foraminifera (alveolinids, nummulitids, and orthophragmines) from the eastern Alborz region (NE Iran): Taxonomy and biostratigraphy implications. Revue de micropaléontologie, 63, 65-84.

Hadi, M., Mosaddegh, H. and Abbassi, N. (2016) Microfacies and biofabric of nummulite accumulations (Bank) from the Eocene deposits of Western Alborz (NW Iran). Journal of African Earth Sciences, 124, 216-233.

Halfar, J. and Mutti, M. (2005) Global dominance of coralline red-algal facies: a response to Miocene oceanographic events. Geology 33, 481–484.

Hallock, P. (1997) Reefs and Reef Limestones in Earth History. In: Birkeland, C. (Ed.), Life and Death of Coral Reefs. Chapman and Hall, New York, pp. 13–42.

Hallock, P. and Seddighi, M. (2022) Why did some larger benthic foraminifera become so large and flat?. Sedimentology, 69(1), 74-87.

Hanif, M., Imraz, M., Ali, F., Haneef, M., Saboor, A., Iqbal, S. and Ahmad, S. (2014) The inner ramp facies of the Thanetian Lockhart Formation, western Salt Range, Indus Basin, Pakistan. Arabian Journal of Geosciences, 7(11), 4911-4926.

Heidari, A., Mahboubi, A., Moussavi-Harami, R., Gonzalez, L. and Moalemi, S. A. (2014) Biostratigraphy, sequence stratigraphy, and paleoecology of the Lower–Middle Miocene of Northern Bandar Abbas, Southeast Zagros basin in south of Iran. Arabian Journal of Geosciences, 7(5), 1829-1855.

Herbert, T.D., Lawrence, K.T., Tzanova, A., Peterson, L.C., Caballero-Gill, R. and Kelly, C.S. (2016) Late Miocene global cooling and the rise of modern ecosystems. Nature Geoscience, 9, 843-847.

Höntzsch, S., Scheibner, C., Guasti, E., Kuss, J., Marzouk, A. M. and Rasser, M. W. (2011) Increasing restriction of the Egyptian shelf during the Early Eocene?—New insights from a southern Tethyan carbonate platform. Palaeogeography, Palaeoclimatology, Palaeoecology, 302(3-4), 349-366.

Hottinger, L. (1982) Larger foraminifera, giant cells with a historical background. Naturwissenschaften, 69(8), 361-371.

Hottinger, L.K. (1983) Neritic Macroid Genesis: an Ecological Approach. In Peryt TM (ed) Coated Grains. Springer-Verlag, Berlin, pp 38-55.

Hu, X., Garzanti, E., Wang, J., Huang, W., An, W. and Webb, A. (2016) The timing of India-Asia collision onset–Facts, theories, controversies. Earth-Science Reviews, 160, 264-299.

Hussein, A. W. (2019) Cyclic hierarchy and depositional sequences of the Middle-Upper Eocene ramp facies: An example from Beni Suef area, east Nile Valley, Egypt. Journal of African Earth Sciences, 149, 307-333.

Hussein, D., Collier, R., Lawrence, J. A., Rashid, F., Glover, P. W. J., Lorinczi, P. and Baban, D. H. (2017) Stratigraphic correlation and paleoenvironmental analysis of the hydrocarbon-bearing Early Miocene Euphrates and Jeribe formations in the Zagros folded-thrust belt. Arabian Journal of Geosciences, 10(24), 1-15.

Ishaq, M., Jan, I. U., Hanif, M. and Awais, M. (2019) Microfacies and diagenetic studies of the early Eocene Sakesar Limestone, Potwar Plateau, Pakistan: approach of reservoir evaluation using outcrop analogue. Carbonates and Evaporites, 34(3), 623-656.

James, N.P. (1997) The cool-water carbonate depositional realm. In: James, N.P., Clarke, J.A.D. (Eds.), Cool-water Carbonates. 56. SEPM Special Publication, pp. 1–22.

Jauhri, A. K., Misra, P. K., Kishore, S. and Singh, S. K. (2006) Larger foraminiferal and calcareous algal facies in the Lakadong Formation of the South Shillong Plateau, NE India. Journal of the Palaeontological Society of India, 51(2), 51-61.

Jiang, J., Hu, X., Li, J., BouDagher-Fadel, M. and Garzanti, E. (2021) Discovery of the Paleocene-Eocene Thermal Maximum in shallow-marine sediments of the Xigaze forearc basin, Tibet: A record of enhanced extreme precipitation and siliciclastic sediment flux. Palaeogeography, Palaeoclimatology, Palaeoecology, 562, 110095.

Johnson, K. G., Jackson, J. B. and Budd, A. F. (2008) Caribbean reef development was independent of coral diversity over 28 million years. Science, 319(5869), 1521-1523.

Joudaki, M., Asnavandi, H., Panah, F. M. and Baghbani, D. (2020) The regional facies analysis and depositional environments of the Oligocene and Lower Miocene deposits; Zagros Basin, SW of Iran. Carbonates and Evaporites, 35(2), 1-18.

Kahsnitz, M. (2017) Paleocene to Lower Eocene sediments of the eastern Neo-Tethyan Ocean: sedimentary and geodynamic evolution as well as biostratigraphy of the larger benthic foraminifera Lockhartia and the genesis of nodular limestones (Doctoral dissertation, Universität Bremen).

Kamran, M., Frontalini, F., Xi, D., Papazzoni, C. A., Jafarian, A., Latif, K., Jiang, T., Mirza, K., Song, H. and Wan, X. (2021) Larger benthic foraminiferal response to the PETM in the Potwar Basin (Eastern Neotethys, Pakistan). Palaeogeography, Palaeoclimatology, Palaeoecology, 575, 110450.

Khan, M., Khan, M. A., Shami, B. A. and Awais, M. (2018) Microfacies analysis and diagenetic fabric of the Lockhart Limestone exposed near Taxila, Margalla Hill Range, Punjab, Pakistan. Arabian Journal of Geosciences, 11(2), 1-15.

Khitab, U., Umar, M. and Jamil, M. (2020) Microfacies, diagenesis and hydrocarbon potential of Eocene carbonate strata in Pakistan. Carbonates and Evaporites, 35(3), 1-15.

Kuss, J. and Boukhary, M. A. (2008) A new upper Oligocene marine record from northern Sinai (Egypt) and its paleogeographic context. GeoArabia, 13(1), 59-84.

Langer, M. R. and Hottinger, L. (2000) Biogeography of selected" larger" foraminifera. Micropaleontology, 46, 105-126.

Less, G., Frijia, G., Özcan, E., Saraswati, P. K., Parente, M. and Kumar, P. (2018) Nummulitids, lepidocyclinids and Sr-isotope data from the Oligocene of Kutch (western India) with chronostratigraphic and paleobiogeographic evaluations. Geodinamica Acta, 30(1), 183-211.

Leutenegger, S. (1984) Symbiosis in benthic foraminifera; specificity and host adaptations. The Journal of Foraminiferal Research, 14, 16-35.

Li, J., Hu, X., Garzanti, E., An, W. and Wang, J. (2015) Paleogene carbonate microfacies and sandstone provenance (Gamba area, South Tibet): Stratigraphic response to initial India–Asia continental collision. Journal of Asian Earth Sciences, 104, 39-54.

Li, J., Hu, X., Zachos, J. C., Garzanti, E. and BouDagher-Fadel, M. (2020) Sea level, biotic and carbon-isotope response to the Paleocene–Eocene thermal maximum in Tibetan Himalayan platform carbonates. Global and Planetary Change, 194, 103316.

Lokier, S. W., Wilson, M. E. and Burton, L. M. (2009) Marine biota response to clastic sediment influx: a quantitative approach. Palaeogeography, Palaeoclimatology, Palaeoecology, 281(1-2), 25-42.

Martín-Martín, M., Guerrera, F., Tosquella, J. and Tramontana, M. (2020) Paleocene-Lower Eocene carbonate platforms of westernmost Tethys. Sedimentary Geology, 404, 105674.

López-Pérez, R. A. (2005) The Cenozoic hermatypic corals in the eastern Pacific: history of research. Earth-Science Reviews, 72(1-2), 67-87.

López-Pérez, A. (2017) Revisiting the Cenozoic history and the origin of the Eastern Pacific coral fauna. In Coral Reefs of the Eastern Tropical Pacific (pp. 39-57). Springer, Dordrecht.

Mahboubi, A., Moussavi-Harami, R., Lasemi, Y. and Brenner, R. L. (2001) Sequence stratigraphy and sea level history of the upper Paleocene strata in the Kopet-Dagh basin, northeastern Iran. AAPG bulletin, 85(5), 839-859.

Mahyad, M., Safari, A., Vaziri-Moghaddam, H. and Seyrafian, A. (2019) Biofacies, taphofacies, and depositional environments in the north of Neotethys Seaway (Qom Formation, Miocene, Central Iran). Russian Geology and Geophysics, 60(12), 1368-1384.

Mattern, F. and Bernecker, M. (2019) A shallow marine clinoform system in limestones (Paleocene/Eocene Jafnayn Formation, Oman): geometry, microfacies, environment and processes. Carbonates and Evaporites, 34(1), 101-113.

Marshall, A. T. and Clode, P. (2004) Calcification rate and the effect of temperature in a zooxanthellate and an azooxanthellate scleractinian reef coral. Coral reefs, 23(2), 218-224.

Miller, K. G., Browning, J. V., Schmelz, W. J., Kopp, R. E., Mountain, G. S. and Wright, J. D. (2020) Cenozoic sea-level and cryospheric evolution from deep-sea geochemical and continental margin records. Science advances, 6(20), eaaz1346.

Moghaddam, H. V., Seyrafian, A. and Taraneh, P. (2002) Biofacies and sequence stratigraphy of the Eocene succession, at Hamzeh-Ali area, north-central Zagros, Iran. Carbonates and Evaporites, 17(1), 60-67.

Mohammadi, E. (2020) Sedimentary facies and depositional environments of the Oligocene–early Miocene marine Qom Formation, Central Iran Back-Arc Basin, Iran (northeastern margin of the Tethyan Seaway). Carbonates and Evaporites, 35(1), 1-29.

Mohammadi, E., Hasanzadeh-Dastgerdi, M., Ghaedi, M., Dehghan, R., Safari, A., Vaziri-Moghaddam, H., Baizidi, C., Vaziri, M. and Sfidari, E. (2013) The Tethyan Seaway Iranian Plate Oligo-Miocene deposits (the Qom Formation): distribution of Rupelian (Early Oligocene) and evaporate deposits as evidences for timing and trending of opening and closure of the Tethyan Seaway. Carbonate Evaporite 28:321–345.

Mohammadi, E., Safari, A., Vaziri-Moghaddam, H., Vaziri, M. R. and Ghaedi, M. (2011) Microfacies analysis and paleoenviornmental interpretation of the Qom Formation, South of the Kashan, Central Iran. Carbonates and Evaporites, 26(3), 255-271.

Mossadegh, Z. K., Haig, D. W., Allan, T., Adabi, M. H. and Sadeghi, A. (2009) Salinity changes during late Oligocene to early Miocene Asmari formation deposition, Zagros mountains, Iran. Palaeogeography, Palaeoclimatology, Palaeoecology, 272(1-2), 17-36.

Nafarieh, E., Boix, C., Cruz-Abad, E., Ghasemi-Nejad, E., Tahmasbi, A. and Caus, E. (2019) Imperforate larger benthic foraminifera from shallow-water carbonate facies (middle and late Eocene), Zagros Mountains, Iran. Journal of Foraminiferal Research, 49(3), 275-302.

Nafarieh, E., Vaziri-Moghaddam, H., Taheri, A. and Ghabeishavi, A. (2012) Biofacies and palaeoecology of the Jahrum Formation in Lar area, Zagros Basin, (SW Iran). Iranian Journal of Science and Technology, 36(A1), 51.

Naveed, A. and Chaudhry, M. N. (2008) Geology of Hettangian to middle Eocene rocks of Hazara and Kashmir basins, Northwest lesser Himalayas, Pakistan. Geological Bulletin of Panjab University, 43, 131-152.

Nebelsick, J. H., Rasser, M. W. and Bassi, D. (2005) Facies dynamics in Eocene to Oligocene circumalpine carbonates. Facies, 51(1), 197-217.

Noorian, Y., Moussavi-Harami, R., Reijmer, J. J., Mahboubi, A., Kadkhodaie, A. and Omidpour, A. (2021) Paleo-facies distribution and sequence stratigraphic architecture of the Oligo-Miocene Asmari carbonate platform (southeast Dezful Embayment, Zagros Basin, SW Iran). Marine and Petroleum Geology, 128, 105016.

Özcan, E., Hanif, M., Ali, N. and Yücel, A. O. (2015) Early Eocene orthophragminids (Foraminifera) from the type-locality of Discocyclina ranikotensis Davies, 1927, Thal, NW Himalayas, Pakistan: insights into the orthophragminid palaeobiogeography. Geodinamica Acta, 27(4), 267-299.

Özcan, E., Saraswati, P. K., Yücel, A. O., Ali, N. and Hanif, M. (2018) Bartonian orthophragminids from the Fulra Limestone (Kutch, W India) and coeval units in Sulaiman Range, Pakistan: a synthesis of shallow benthic zone (SBZ) 17 for the Indian Subcontinent. Geodinamica acta, 30(1), 137-162.

Pomar, L. and Hallock, P. (2007) Changes in coral-reef structure through the Miocene in the Mediterranean province: adaptive versus environmental influence. Geology, 35(10), 899-902.

Pomar, L., Brandano, M. and Westphal, H. (2004) Environmental factors influencing skeletal grain sediment associations: a critical review of Miocene examples from the western Mediterranean. Sedimentology, 51(3), 627-651.

Pomar, L., Bassant, P., Brandano, M., Ruchonnet, C. and Janson, X. (2012) Impact of carbonate producing biota on platform architecture: insights from Miocene examples of the Mediterranean region. Earth-Science Reviews, 113(3-4), 186-211.

Pomar, L., Baceta, J.I., Hallock, P., Mateu-Vicens, G. and Basso, D. (2017) Reef building and carbonate production modes in the west-central Tethys during the Cenozoic. Mar. Pet. Geol. 83, 261–304.

Perrin, C. (1992) Signification écologique des foraminifères acervulinidés et leur rôle dans la formation de faciès récifaux et organogènes depuis le Paléocène. Geobios, 25(6), 725-751.

Perrin, C. (2009) Solenomeris: from biomineralization patterns to diagenesis. Facies, 55(4), 501-522.

Perrin, C. and Bosellini, F. R. (2012) Paleobiogeography of scleractinian reef corals: changing patterns during the Oligocene–Miocene climatic transition in the Mediterranean. Earth-Science Reviews, 111(1-2), 1-24.

Perrin, C. and Kiessling, W. (2012) Latitudinal trends in Cenozoic reef patterns and their relationship to climate. In: Mutti, M., Piller, W., Betzler, C. (Eds.), Carbonate Systems during the Oligocene-Miocene Climatic Transition, vol. 42. Wiley-Blackwell, Oxford, UK, International Association of Sedimentologists Special Publications, pp. 17–34.

Perry, O.R. and Choquette, P.W. (1985) Carbonate petroleum reservoirs. Springer, New York.

Rahmani, A., Vaziri-Moghaddam, H., Taheri, A. and Ghabeishavi, A. (2009) A model for the paleoenvironmental distribution of larger foraminifera of Oligocene–Miocene carbonate rocks at Khaviz Anticline, Zagros Basin, SW Iran. Historical Biology, 21(3-4), 215-227.

Rasser W.M. (1994) Facies and palaeoecology of rhodoliths and acervulinid macroids in the Eocene of the Krappfeld (Austria). Beitr. Paläont., 19: 191-217.

Rasser, M.W. and Piller, W.E. (1997) Depth distribution of calcareous encrusting associations in the northern Red Sea (Safaga, Egypt) and their geological implications. Proceedings of the 8th international Coral Reef Symposium, 743-748.

Renema, W. (2018) Terrestrial influence as a key driver of spatial variability in large benthic foraminiferal assemblage composition in the Central Indo-Pacific. Earth-Science Reviews, 177, 514-544.

Reuter, M., Piller, W.E., Harzhauser, M., Mandic, O., Berning, B., Rogl, F., Kroh, A., Aubry, M.P., Wielandt-Schuster, U. and Hamedani, A. (2009) The Oligo-/Miocene Qom Formation (Iran): evidence

for an early Burdigalian restriction of the Tethyan Seaway and closure of its Iranian gateways. International Journal of Earth Sciences 98 (3), 627–650. doi:10.1007/s00531-007-0269-9.

Reuter, M., Piller, W. E., Harzhauser, M., Kroh, A. and Bassi, D. (2008) Termination of the Arabian shelf sea: Stacked cyclic sedimentary patterns and timing (Oligocene/Miocene, Oman). Sedimentary Geology, 212(1-4), 12-24.

Riosmena-Rodríguez, R. (2017) Natural History of Rhodolith/Maërl Beds: Their role in near-shore biodiversity and management. In: Riosmena-Rodríguez R., Nelson W. & Aguirre J. (Eds) - Rhodolith/Maërl Beds: A Global Perspective. Coastal Research Library, 15: 3-27. Springer.

Robertson, A.H.F., Parlak, O. and Ustaömer, T. (2012) Overview of the Palaeozoic–Neogene evolution of Neotethys in the Eastern Mediterranean region (Southern Turkey, Cyprus, Syria). Petroleum Geosciences, 18, 381-404.

Rögl, F. (1999) Mediterranean and Paratethys facts and hypotheses of an Oligocene to Miocene paleogeography (short overview). Geologica Carpathica. 50. 339-349.

Roozpeykar, A. and Moghaddam, I. M. (2016) Benthic foraminifera as biostratigraphical and paleoecological indicators: an example from Oligo-Miocene deposits in the SW of Zagros basin, Iran. Geoscience Frontiers, 7(1), 125-140.

Rosenfeld, A. and Hirsch, F. (2005) The Paleocene – Eocene of Israel, in: Hall, J.K., Krasheninnikov, V.A., Hirsch, F., Benjamini, C., Flexer, A. (Eds.), Geological Framework of the Levant - Volume II: The Levantine Basin and Israel. Historical Productions-Hall, Jerusalem, pp. 437–458.

Sadeghi, R., Vaziri-Moghaddam, H. and Taheri, A. (2011) Microfacies and sedimentary environment of the Oligocene sequence (Asmari Formation) in Fars sub-basin, Zagros Mountains, southwest Iran. Facies, 57(3), 431-446.

Safari, A., Ghanbarloo, H., Mansoury, P. and Esfahani, M. M. (2020) Reconstruction of the depositional sedimentary environment of Oligocene deposits (Qom Formation) in the Qom Basin (northern Tethyan seaway), Iran. Geologos, 26(2), 93-111.

Sadooni, F. N. and Alsharhan, A. S. (2019) Regional stratigraphy, facies distribution, and hydrocarbons potential of the Oligocene strata across the Arabian Plate and Western Iran. Carbonates and Evaporites, 34(4), 1757-1770.

Sallam, E., Wanas, H. A. and Osman, R. (2015) Stratigraphy, facies analysis and sequence stratigraphy of the Eocene succession in the Shabrawet area (north Eastern Desert, Egypt): an example for a tectonically influenced inner ramp carbonate platform. Arabian Journal of Geosciences, 8(12), 10433-10458.

Sarkar, S. (2016) Early Eocene calcareous algae and benthic foraminifera from Meghalaya, NE India: A new record of microfacies and palaeoenvironment. Journal of the Geological Society of India, 88(3), 281-294.

Sarkar, S. (2017) Microfacies analysis of larger benthic foraminifera-dominated Middle Eocene carbonates: a palaeoenvironmental case study from Meghalaya, NE India (Eastern Tethys). Arabian Journal of Geosciences, 10(5), 1-13.

Sarkar, S. (2018) The enigmatic Palaeocene-Eocene coralline *Distichoplax*: Approaching the structural complexities, ecological affinities and extinction hypotheses. Marine Micropaleontology, 139, 72-83.

Scotese, C.R. (2014) a Atlas of Paleogene Paleogeographic Maps (Mollweide Projection), Maps 8-15, Volume 1, The Cenozoic, PALEOMAP Atlas for ArcGIS, PALEOMAP Project, Evanston, IL.

Scotese, C.R. (2014) b Atlas of Neogene Paleogeographic Maps (Mollweide Projection), Maps 1-7, Volumes 1, The Cenoaoic, PALEOMAP Atlas for ArcGIS, PALEOMAP Project, Evanston, IL.

Schaub, H., Benjamini, C. and Moshkovitz, S. (1995) The Biostratigraphy of the Eocene of Israel: Nummulites, Planktic Foraminifera and Calcareous Nannofossils. Kommission der Schweizerischen Paläontologischen Abhandlungen, 58p.

Scheibner, C., Kuss, J. and Marzouk, A. M. (2000) Slope sediments of a Paleocene ramp-to-basin transition in NE Egypt. International Journal of Earth Sciences: Geologische Rundschau, 88(4), 708.

Scheibner, C., Reijmer, J. J. G., Marzouk, A. M., Speijer, R. P. and Kuss, J. (2003) From platform to basin: the evolution of a Paleocene carbonate margin (Eastern Desert, Egypt). International Journal of Earth Sciences, 92(4), 624-640.

Scheibner, C. and Speijer, R. P. (2008) Late Paleocene–early Eocene Tethyan carbonate platform evolution - A response to long-and short-term paleoclimatic change. Earth-Science Reviews, 90(3-4), 71-102.

Schlager, W. (2003) Benthic carbonate factories of the Phanerozoic. Int. J. Earth Sci. 92, 445–464.

Seyrafian, A. and Toraby, H. (2005) Petrofacies and sequence stratigraphy of the Qom Formation (Late Oligocene-Early Miocene?), north of Nain, southern trend of central Iranian Basin. Carbonates and Evaporites, 20(1), 82-90.

Serra-Kiel, J., Hottinger, L., Caus, E., Drobne, K., Ferrandez, C., Jauhri, A.K., Less, G., Pavlovec, R., Pignatti, J., Samso, J.M., Schaub, H., Sirel, E., Strougo, A., Tambareau, Y., Tosquella, J. and Zakrevskaya, E. (1998) Larger foraminiferal biostratigraphy of the Tethyan. Bulletin de la Société géologique de France, 169, 281-299.

Shabafrooz, R., Mahboubi, A., Vaziri-Moghaddam, H., Ghabeishavi, A. and Moussavi-Harami, R. (2015) Depositional architecture and sequence stratigraphy of the oligo–miocene Asmari platform; Southeastern Izeh zone, Zagros Basin, Iran. Facies, 61(1), 1-32.

Sissakian, V. K. (2013) Geological evolution of the Iraqi Mesopotamia Foredeep, inner platform and near surroundings of the Arabian Plate. Journal of Asian Earth Sciences, 72, 152-163.

Stanley, S. M. (2006) Influence of seawater chemistry on biomineralization throughout Phanerozoic time: Paleontological and experimental evidence. Palaeogeography, Palaeoclimatology, Palaeoecology, 232(2-4), 214-236.

Steinthorsdottir, M., Coxall, H.K., de Boer, A.M., Huber, M., Barbolini, N., Bradshaw, C.D., Burls, N.J., Feakins, S.J., Gasson, E., Henderiks, J., Holbourn, A., Kiel, S., Kohn, M.J., Knorr, G., Kürschner, W.M., Lear, C., Liebrand, D., Lunt, D.J., Mörs, T., Pearson, P.N., Pound, M.J., Stoll, H. and

Strömberg, C.A.E. (2020) The Miocene: the Future of the Past. Paleoceanography and Paleoclimatology, e2020PA004037.

Swati, M. A. F., Haneef, M., Ahmad, S., Naveed, Y., Zeb, W., Akhtar, N. and Owais, M. (2013) Biostratigraphy and depositional environments of the Early Eocene Margalla Hill Limestone, Kohala-Bala area, Haripur, Hazara Fold-Thrust Belt, Pakistan. Journal of Himalayan Earth Sciences, 46(2), 65.

Taheri, A., Vaziri-Moghaddam, H. and Seyrafian, A. (2008) Relationships between foraminiferal assemblages and depositional sequences in Jahrum Formation, Ardal area (Zagros Basin, SW Iran). Historical Biology, 20(3), 191-201.

Titelboim, D., Almogi-Labin, A., Herut, B., Kucera, M., Asckenazi-Polivoda, S. and Abramovich, S. (2019) Thermal tolerance and range expansion of invasive foraminifera under climate changes. Scientific reports, 9(1), 1-5.

Tomás, S., Frijia, G., Bömelburg, E., Zamagni, J., Perrin, C. and Mutti, M. (2016) Evidence for seagrass meadows and their response to paleoenvironmental changes in the early Eocene (Jafnayn Formation, Wadi Bani Khalid, N Oman). Sedimentary Geology, 341, 189-202.

Torfstein, A. and Steinberg, J. (2020) The Oligo–Miocene closure of the Tethys Ocean and evolution of the proto-Mediterranean Sea. Scientific reports, 10(1), 1-10.

Tucker, M.E. and Wright, V.P. (1990) Carbonate Sedimentology. Blackwell, Oxford, pp. 1–496.

Van Buchem, F.S.P., Allan, T.L., Laursen, G.V., Lotfpour, M., Moallemi, A., Monibi, S., Motiei, H., Pickard, N.A.H., Tahmasbi, A.R., Vedrenne, V. and Vincent, B. (2010) Regional stratigraphic architecture and reservoir types of the Oligo-Miocene deposits in the Dezful Embayment (Asmari and Pabdeh Formations) SW Iran. In: Van Buchem, F.S.P., Gerdes, K.D., Esteban, M. (Eds.), Mesozoic and Cenozoic Carbonate Systems of the Mediterranean and the Middle East: Stratigraphic and Diagenetic Reference Models: Geological Society, London, Special Publications, London, pp. 219–263.

Vaziri-Moghaddam, H., Kalanat, B. and Taheri, A. (2011) Sequence stratigraphy and depositional environment of the Oligocene deposits at Firozabad section, southwest of Iran based on microfacies analysis. Geopersia, 1(1), 71-152.

Vaziri-Moghaddam, H., Kimiagari, M. and Taheri, A. (2006) Depositional environment and sequence stratigraphy of the Oligo-Miocene Asmari Formation in SW Iran. Facies, 52(1), 41-51.

Vaziri-Moghaddam, H., Seyrafian, A., Taheri, A. and Motiei, H. (2010) Oligocene-Miocene ramp system (Asmari Formation) in the NW of the Zagros basin, Iran: Microfacies, paleoenvironment and depositional sequence. Revista mexicana de ciencias geológicas, 27(1), 56-71.

Willems, H., Zhou, Z., Zhang, B. G. and Gräfe, K. U. (1996) Stratigraphy of the Upper Cretaceous and lower Tertiary strata in the Tethyan Himalayas of Tibet (Tingri area, China). Geologische Rundschau, 85(4), 723-754.

Wilson, M.E.J. (2008) Global and regional influences on equatorial shallow-marine carbonates during the Cenozoic. Palaeogeogr. Palaeoclimatol. Palaeoecol. 265, 262–274.

Wilson, M. E. J. and Vecsei, A. (2005) The apparent paradox of abundant foramol facies in low latitudes: their environmental significance and effect on platform development. Earth-Science Reviews, 69(1-2), 133-168.

Whittle, G. L., Alsharhan, A. S. and El Deeb, W. M. Z. (1995) Bio-lithofacies and diagenesis in the early-middle oligocene of Abu Dhabi, United Arab Emirates. Carbonates and Evaporites, 10(1), 54-64.

Wright, V.P. and Burchette, T.P. (1996) Shallow-water carbonate environments. In: Reading, H.G. (Ed.), Sedimentary Environments. Blackwell, Oxford, pp. 325–394.

Yazdi-Moghadam, M., Sadeghi, A., Adabi, M. H. and Tahmasbi, A. (2018) a. Foraminiferal biostratigraphy of the lower Miocene Hamzian and Arashtanab sections (NW Iran), northern margin of the Tethyan Seaway. Geobios, 51(3), 231-246.

Yazdi-Moghadam M., Sadeghi A., Adabi M.H. and Tahmasbi A. (2018) b. Stratigraphy of the lower Oligocene nummulitic limestones, north of Sonqor (Nw Iran) Riv. It. Paleontol. Strat., 124(2): 407-416.

Yazdi-Moghadam, M., Sarfi, M., Ghasemi-Nejad, E., Sadeghi, A. and Sharifi, M. (2021) Early Miocene larger benthic foraminifera from the northwestern Tethyan Seaway (NW Iran): new findings on Shallow Benthic Zone 25. International Journal of Earth Sciences, 110(2), 719-740.

Yousefi-Yegane, B. (2019) Facies and paleoenvironmental reconstruction of Early–Middle Miocene deposits in the north-west of the Zagros Basin, Iran. Geologica Carpathica, 70(1), 75-87.

Zachos, J., Pagani, M., Sloan, L., Thomas, E. and Billups, K. (2001) Trends, rhythms, and aberrations in global climate 65 Ma to present. Science, 292(5517), 686-693.

Ziegler, A. M. (2001) Late Permian to Holocene paleofacies evolution of the Arabian Plate and its hydrocarbon occurrences. GeoArabia, 6(3), 445-504.

Zhang, Q., Willems, H. and Ding, L. (2013) Evolution of the Paleocene-Early Eocene larger benthic foraminifera in the Tethyan Himalaya of Tibet, China. International Journal of Earth Sciences, 102(5), 1427-1445.

Zoeram, F. Z., Vahidinia, M., Sadeghi, A., Mahboubi, A. and Bakhtiar, H. A. (2015) Larger benthic foraminifera: a tool for biostratigraphy, facies analysis and paleoenvironmental interpretations of the Oligo-Miocene carbonates, NW Central Zagros Basin, Iran. Arabian Journal of Geosciences, 2(8), 931-949.

Zohdi, A., Mousavi-Harami, R., Ali Moallemi, S., Mahboubi, A. and Immenhauser, A. (2013) Evolution, paleoecology and sequence architecture of an Eocene carbonate ramp, southeast Zagros Basin, Iran. GeoArabia, 18(4), 49-80.